performance in the T-maze delayed alternation task in rats. Phytother. Res. 7, 49–52.

Nitta, H., Matsumoto, K., Shimizu, M., Ni, X.H., Watanabe, H., 1995a. Panax Ginseng extract improves the performance of aged Fischer 344 rats in radial maze task but not in operant brightness discrimination task. Biol. Pharm. Bull. 18, 1286–1288.

Nitta, H., Matsumoto, K., Shimizu, M., Ni, X.-H., Watanabe, H., 1995b. Panax Ginseng extract improves the scopolamine-induced disruption of 8-arm radial maze performance in rats. Biol. Pharm. Bull. 18, 1439–1442.

Nowakowski, R.S., Lewin, S.B., Miller, M.W., 1989. Bromodeoxyuridine immunohistochemical determination of the lengths of the cell cycle and the DNA-synthetic phase for an anatomically defined population. J. Neurocytol. 18, 311–318.

Packard Jr., D.S., Menzies, R.A., Skalko, R.G., 1973. Incorporation of thymidine and its analogue, bromodeoxyuridine, into embryos and maternal tissues of the mouse. Differentiation 1, 397–404.

Paxinos, G., Watson, C., 1986. The Rat Brain in Stereotaxic Coordinates. Academic Press, San Diego.

Petkov, V.D., Mosharrof, A.H., Petkov, V.V., Kehayov, R.A., 1990. Age-related differences in memory and in the memory effects of nootropic drugs. Acta Physiol. Pharmacol. Bulg. 16, 28–36.

Petkov, V.D., Cao, Y., Todorov, I., Lazarova, M., Getova, D., Stancheva, S., Alova, L., 1992. Behavioral effects of stem-leaves extracts from Panax Ginseng C.A. Meyer. Acta Physiol. Pharmacol. Bulg. 18, 41–48.

Petkov, V.D., Kehayov, R., Belcheva, S., Konstantinova, E., Petkov, V.V., Getova, D., Markovska, V., 1993. Memory effects of standardized extracts of Panax Ginseng (G115) Ginkgo biloba (GK501) and their combination Gincosan (PHL-00701). Planta Med. 59, 106–114.

Saito, H., Tsuchiya, M., Naka, S., Takagi, K., 1977. Effects of Panax Ginseng root on conditioned avoidance response in rats. Jpn. J. Pharmacol. 27, 509–516.

Saito, H., Tsuchiya, M., Naka, S., Takagi, K., 1979. Effects of Panax Ginseng root on acquisition of sound discrimination behavior in rats. Jpn. J. Pharmacol. 29, 319–324.

Salim, K.N., McEwen, B.S., Chao, H.M., 1997. Ginsenoside Rb1 regulates ChAT, NGF and trkA mRNA expression in the rat brain.. Brain Res. Mol. Brain Res. 47, 177–182.

Shan, S.J., Xu, Q.P., Shoyama, Y., 2002. Extract of Yi Zhi Fang improves learning and memory behaviours of mice and its possible mechanisms. Phytother. Res. 5, 449–454.

Silva, A.J., Kogan, J.H., Frankland, P.W., Kida, S., 1998. CREB and memory. Annu. Rev. Neurosci. 21, 127–148.

Vaccarino, F.M., Hayward, M.D., Le, H.N., Hartigan, D.J., Duman, R.S., Nestler, E.J., 1993. Induction of immediate early genes by cyclic AMP in primary cultures of neurons from rat cerebral cortex.. Brain Res. Mol. Brain Res. 19, 76–82.

Wang, B.X., Cui, J.C., Liu, A.J., Wu, S.K., 1983. Studies on the anti-fatigue effect of the saponins of stems and leaves of Panax Ginseng (SSLG). J. Tradit. Chin. Med. 3, 89–94.

Watanabe, H., Ohta, H., Matsumoto, K., 1990. Effect of Ginseng on spontaneous motor activity, water maze learning and central dopaminergic systems in old rats. In: Shibata, S., Ohtsuka, Y., Saito, H. (Eds.), Recent Advances in Ginseng Studies. Tokyo Hirokawa, Tokyo, pp. 73–81.

Wen, T.C., Yoshimura, H., Matsuda, S., Lim, J.H., Sakanaka, M., 1996. Ginseng root prevents learning disability and neuronal loss in gerbils with 5-min forebrain ischemia. Acta Neuropathol. 91, 15–22.

Yoshimura, H., Watanabe, K., Ogawa, N., 1998. Psychotropic effects of Ginseng saponins on agonistic behavior between resident and intruder mice. Eur. J. Pharmacol. 146, 291–297.

Zhao, R., McDaniel, W.F., 1998. Ginseng improves strategic learning by normal and brain-damaged rats. Neuroreport 9, 1619–1624.

Zhong, Y.M., Nishijo, H., Uwano, T., Yamaguchi, H., Ono, T., 1998. Red Ginseng ameliorates place learning deficits in aged rats and in young rats with selective hippocampal lesions. In: Proceedings of the Seventh International Symposium on Ginseng. pp. 1–11.

THE JOURNAL OF BIOLOGICAL CHEMISTRY
Vol. 278, No. 20, Issue of May 16, pp. 18597–18605, 2003
Printed in U.S.A.

Molecular Cloning and Characterization of CLICK-III/CaMKIγ, a Novel Membrane-anchored Neuronal Ca^{2+}/Calmodulin-dependent Protein Kinase (CaMK)*

Received for publication, January 17, 2003, and in revised form, February 26, 2003
Published, JBC Papers in Press, March 11, 2003, DOI 10.1074/jbc.M300578200

Sayaka Takemoto-Kimura‡§, Hisashi Terai‡, Maki Takamoto‡¶, Shogo Ohmae‡, Shoko Kikumura‡, Eri Segi‡‖, Yoshiki Arakawa‡§, Tomoyuki Furuyashiki‡‖, Shuh Narumiya‡, and Haruhiko Bito‡¶‡‡**

*From the ‡Department of Pharmacology, Kyoto University Faculty of Medicine, ¶PRESTO-Japan Science and Technology Corporation, Sakyo-ku, Kyoto 606-8315, and **Department of Neurochemistry, University of Tokyo Graduate School of Medicine, Bunkyo-ku, Tokyo 113-0033, Japan*

During a screen for novel putative Ca^{2+}/calmodulin-dependent protein kinase (CaMK)-like CREB kinases (CLICKs), we have cloned a full-length cDNA for CLICK-III/CaMKIγ, an isoform of the CaMKI family with an extended C-terminal domain ending with *CAAX* motif (where *AA* is aliphatic acid). As expected from the similarity of its kinase domain with the other CaMKI isoforms, full activation of CLICK-III/CaMKIγ required both Ca^{2+}/CaM and phosphorylation by CaMKK. We also found that Ca^{2+}/cAMP-response element-binding protein (CREB) was a good substrate for CLICK-III/CaMKIγ, at least *in vitro*. Interestingly enough, CLICK-III/CaMKIγ transcripts were most abundant in neurons, with the highest levels in limited nuclei such as the central nucleus of the amygdala (CeA) and the ventromedial hypothalamus. Consistent with the presence of the *CAAX* motif, CLICK-III/CaMKIγ was found to be anchored to various membrane compartments, especially to Golgi and plasma membranes. Both point mutation in the *CAAX* motif and treatment with compactin, a 3-hydroxy-3-methylglutaryl-coenzyme A reductase inhibitor, disrupted such membrane localization, suggesting that membrane localization of CLICK-III/CaMKIγ occurred in a prenylation-dependent way. These findings provide a novel mechanism by which neuronal CaMK activity could be targeted to specific membrane compartments.

Neuronal Ca^{2+} is known to play a critical role as an intracellular second messenger, linking neuronal excitability with many kinds of cellular biological events including synaptic plasticity and neuronal cell survival/apoptosis (1–4). One of the unique features of Ca^{2+} is that its concentration can be dynamically regulated both temporally and spatially (5). Despite a growing knowledge about the critical molecules involved in neuronal Ca^{2+} influx and mobilization (*e.g. N*-methyl-D-aspartic acid receptors, voltage-gated Ca^{2+} channels, inositol 1,4,5-trisphosphate receptors, and ryanodine receptors), how these are converted to the specific cellular events remains largely unknown.

A significant part of signaling downstream Ca^{2+} is thought to be mediated by calmodulin (CaM),[1] a ubiquitous and evolutionary well conserved intracellular Ca^{2+} receptor (6, 7). Although a large number of molecules have been shown to be targeted and activated by the Ca^{2+}/CaM complex, one subgroup of multifunctional kinases, Ca^{2+}/calmodulin-dependent protein kinases (CaMKs), has been ascribed a prominent role. This is because several unique characteristics of this group of kinases, such as rapid activation by Ca^{2+}, steep Ca^{2+}/CaM dependence, and induction of an autonomous kinase activity following activation, render its members good candidates as molecular devices able to convert a transient burst of synaptic activity into a longer lasting covalent modification of substrate proteins (8–15). Indeed, among the CaMK family members, CaMKIIα and β isoforms, which are present postsynaptically and presynaptically, have been implicated in various kinds of synaptic plasticity and homeostasis (8–11), whereas a CaMKK/CaMKIV cascade has been shown to couple synaptic stimuli with CREB-dependent gene expression (4, 12, 16). The ability of the CaMKI isoforms and a related kinase, CKLiK, to phosphorylate neuronal substrates, such as synapsin I and CREB *in vitro*, has been demonstrated so far (13, 17, 18). However, little is yet known about the physiological role of CaMKI, although CaMKIα and CaMKIβ have been shown to be expressed both in neural as well as non-neural peripheral tissues (13, 17–21).

In this study, we report the molecular cloning of mouse full-length CLICK-III/CaMKIγ (occasionally abbreviated to CLICK-III in this paper), an isoform of CaMKI family, that has a longer C-terminal region terminating with a *CAAX* motif (where *AA* is aliphatic acid). This motif has been shown to be conjugated with isoprenoid lipids, thereby allowing proper tar-

* This work was supported by grants-in-aid from the Ministry of Education, Science, Sports, Culture and Technology, the Ministry of Health, Labor, and Welfare of Japan, a PRESTO investigatorship from the Japan Science and Technology Corp., and grants from the Asahi Glass Foundation, the Human Frontier Science Program, the Narishige Neuroscience Research Foundation, the Tokyo Biochemical Research Foundation, the Ube Research Foundation, and the Yamanouchi Foundation for Research on Metabolic Disorders. The costs of publication of this article were defrayed in part by the payment of page charges. This article must therefore be hereby marked "*advertisement*" in accordance with 18 U.S.C. Section 1734 solely to indicate this fact.

§ Predoctoral fellows from the Japan Society for Promotion of Science.
‖ Postdoctoral fellows from the Japan Society for Promotion of Science.
‡‡ To whom correspondence should be addressed. Tel.: 81-3-5841-3559; Fax: 81-3-3814-8154; E-mail: hbito@m.u-tokyo.ac.jp.

[1] The abbreviations used are: CaM, calmodulin; CaMK, Ca^{2+}/calmodulin-dependent protein kinase; CREB, Ca^{2+}/cAMP-response element-binding protein; CLICKs, CaMK-like CREB kinases; VMH, ventromedial hypothalamus; HMG-CoA, 3-hydroxy-3-methylglutaryl-coenzyme A; RACE, rapid amplification of cDNA ends; HA, hemagglutinin; GFP, green fluorescent protein; EGFP, enhanced GFP; wt, wild type; PBS, phosphate-buffered saline; MBP, myelin basic protein; HBSS, Hanks' balanced salt solution; CNS, central nervous system; CeA, central nucleus of amygdala; CMV, cytomegalovirus.

geting of various signaling molecules to cellular membrane compartments (22, 23). CLICK-III was identified during a screen for novel putative CaMK-like CREB kinases (CLICKs), as a kinase homologous to CLICK-I and CLICK-II (the cloning and characterization of CLICK-I and -II will be described elsewhere).[2]

The kinase activity of CLICK-III was similar in many respects to CaMKIα and related kinases. Thus, full activation of CLICK-III required both Ca^{2+}/CaM and phosphorylation by a CaMKK (24–31). In addition, Ca^{2+}/cAMP-response element-binding protein (CREB) (4, 32) was a good substrate for CLICK-III, at least *in vitro*. Interestingly, CLICK-III transcripts were most abundant in neurons, with the highest levels in limited nuclei such as the central nucleus of the amygdala (CeA) and the ventromedial hypothalamus (VMH). Furthermore, CLICK-III was found to be anchored to membrane compartments, consistent with the presence of the *CAAX* motif at its C-terminal end. A point mutation in the *CAAX* motif and treatment with compactin, a 3-hydroxy-3-methylglutaryl coenzyme A (HMG-CoA) reductase inhibitor (33), disrupted such membrane localization, suggesting that membrane localization of CLICK-III occurred in a prenylation-dependent way. These findings provide a novel mechanism by which neuronal CaMK activity could be targeted to specific membrane compartments.

EXPERIMENTAL PROCEDURES

Cloning and Plasmid Constructions—Human hippocampal cDNA was prepared from poly(A)$^+$ RNA (Clontech) using Omniscript reverse transcriptase (Qiagen) and oligo(dT) primers. An hCLICK-III cDNA was obtained by nested PCR using two primer pairs (F1, 5′-CCA CTC CCT GCA ATA AAG CAT CCT C-3′, and R1, 5′-CTG CCT ATG AGT GGG AGA GGC CTT T-3′ as a first primer set; F2, 5′-TGG AGG CAA TGG GTC GAA AGG AAG AA-3′, and R2, 5′-TGT CCA TTT CTT TCA GTC CTG TTG A-3′ as a nested primer set) and subcloned into pCR-Blunt vector (Invitrogen). ICR mouse hippocampal poly(A)$^+$ RNA was purified using Trizol (Invitrogen) and μMACS mRNA isolation kit (Miltenyl Biotec), and mCLICK-III was subsequently obtained by the 3′-RACE procedure, using SMART RACE cDNA amplification kit (Clontech) following the manufacturer's instructions. A gene-specific 5′-primer for 3′-RACE was designed based on the cDNA sequence of hCLICK-III and that of rat CaMKIγ (19) at the 5′-untranslated region adjacent to the first methionine (5′-GCA GCT TCA ACT CTG GAG G-3′). A single RACE-amplified fragment was obtained and subcloned into pCR-Blunt vector, and its nucleotide sequence was determined. Two independent clones were recovered and yielded an identical sequence. To construct pIRES-HAmCL3wt and pIRES-HAmCL3dC, cDNA fragments were amplified by PCR using primers F and R1 or R2 (F, 5′-GGG GGA ATT CTG GCG GCC GCT ATG GGG CGT AAG GAG GAG GAG-3′, and R1 for wt, 5′-GGG GGA ATT CGT TTG GCG GCC GCC TCC TGG GAT CAC ATA ACG AG-3′, or R2 for dC, 5′-GGG GGA ATT CGT TTG GCG GCC GCA AAG TTC TTC TAA ATC TGG AG-3′) and inserted in-frame downstream to an HA tag cassette at the *Not*I site of pIRES-S-Tag-EGFP vector (a kind gift from Dr. Hirohide Takebayashi). To construct pcDNA3-HAmCL3wt and pcDNA3-HAmCL3dC, *Eco*RV/*Eco*RI fragments of each pIRES-S-Tag-EGFP construct were blunted and subcloned into the *Eco*RV site of pcDNA3 (Invitrogen). To construct pEGFP-mCL3 and pEGFP-mCL3C474S, cDNA fragments amplified with primers F and R1 or R2 (F, 5′-GCT TCG AAT TCA GGC TTC AAC TC-3′, and R1 for wt, 5′-CCC TCC CGC GGT CAC ATA ACG AGA GAC ACC CCA GTC-3′, or R2 for C474S, 5′-CCC TCC CGC GGT CAC ATA ACG AGA CAC ACC CCA GTC-3′) were inserted into a pEGFP-C3 vector (Clontech) cut at *Eco*RI and *Sac*II sites. To construct pEGFP-CLVM, two oligonucleotide pairs (5′-CTG TCT CGT TAT GTG AGT GCA CA-3′ and 5′-GAT CTG TGC ACT CAC ATA ACG AGA CAG GGC C-3′) were annealed, phosphorylated, and inserted to a pEGFP-C2 vector (Clontech) at the *Apa*I and *Bam*HI sites. To construct pd2EGFPN1-CaMKKactiveMyc, a 1.3-kb cDNA fragment encoding the N-terminal kinase domain of rat CaMKKα was PCR-cloned from a Sprague-Dawley rat hippocampal cDNA pool, fused to a Myc epitope tag using a pair of primers (F, 5′-ACG GTA CCA TGG AGC GCA GTC CAG CCG, and R, 5′-ATT GGA TCC CTA CAG GTC CTC CTC GCT GAT CAG CTT CTG CTC TCC ATG CTT GGT CAC CCA-3′), and inserted into a pd2EGFPN1 vector (Clontech) cut at *Kpn*I and *Bam*HI site. To construct pEGFP-rCaMKIα, a cDNA fragment corresponding to the full-length coding region of rat CaMKIα was obtained by PCR using primers (F, 5′-AAC TCGAGT GGG CCA TGC CAG GGG CAG TG-3′, and R, 5′-ATT GGA TCC TAG TCC TAG TCC ATG GCC CTA GAG CT-3′), subcloned into a pBluescriptII KS(+) vector cut at *Xho*I and *Bam*HI sites, and thereafter transferred in-frame to pEGFP-C1 vector (Clontech) at *Eco*RI and *Bam*HI sites. All inserts in the expression vectors were verified by sequencing.

Northern Blotting—For Northern blot analysis, a total RNA blot filter was purchased from Seegene (Mouse Brain Aging Blot), and poly(A)$^+$ RNA blot filters were from Clontech (all other blots). Double-stranded probe templates, corresponding to the unique sequence of CLICK-III at the C-terminal region, were generated by PCR using primers (F, 5′-AAG CCT CAG AAA CCT CTA GAC CCA G-3′, and R, 5′-TTC AGA CCC AAG CTG GGG CTC CAT CT-3′ for hCLICK-III; F, 5′-ATG AAC CTG CAC AGC CCC AGT G-3′, and R, 5′-TTA TTG GCC TTT CTG AAG AGG-3′ for mCLICK-III). The probes were labeled with [α-^{32}P]dCTP using Ready-to-Go DNA labeling beads (Amersham Biosciences) and hybridized with the filters in ExpressHyb Hybridization Solution (Clontech) at 68 °C. The filters were washed four times in 0.05% SDS, 2× SSC for 10 min at 50 °C, washed once in 0.1% SDS, 0.1× SSC for 40 min at 50 °C, and subjected to x-ray film autoradiography.

In Situ Hybridization—Brain cryosections (10 μm) were obtained from 2-month-old female ICR mice and processed for *in situ* hybridization as described previously (34). N-terminal (231 bp) and C-terminal (374 bp) fragments were amplified by PCR (5′-GCA GCT TCA ACT CTG GAG G-3′ and 5′-TAG GCT GCT GTC CCG GAA GG-3′ for N-terminal fragment, 5′-ATG AAC CTG CAC AGC CCC AGT G-3′ and 5′-TTA TTG GCC TTT CTG AAG AGG-3′ for C-terminal fragment) and subcloned into pBluescriptII KS(+) vector at the *Sac*II site. [^{35}S]-Labeled riboprobes were generated using T7 RNA polymerase (Stratagene) and [α-^{35}S]CTP.

CaM-Sepharose Binding Assay—COS-7 cells were maintained in Dulbecco's modified Eagle medium containing 10% fetal calf serum. Cells were subcultured in 6-cm dishes 12 h before transfection. pcDNA3-HAmCL3wt (2 μg) or empty vector (2 μg) were transfected using 4 μl of LipofectAMINE 2000 reagent (Invitrogen). After 24 h, the cells were washed twice with ice-cold PBS(−) and lysed in lysis buffer containing 50 mM Tris-HCl (pH 8.0), 150 mM NaCl, 2 mM $CaCl_2$, 1% Triton X-100, 0.5% deoxycholate, and protease inhibitors (Complete tablet, Roche Applied Science). After the protein concentrations were determined using a DC protein assay kit (Bio-Rad), 250 μg of the lysates were incubated with 15 μl of CaM-Sepharose (Amersham Biosciences) in the lysis buffer for 2 h at 4 °C. Beads were washed for six times in the lysis buffer or Ca^{2+}-free lysis buffer containing 50 mM Tris-HCl (pH 8.0), 150 mM NaCl, 2 mM EGTA, 1% Triton X-100, 0.5% deoxycholate, and protease inhibitors. CaM-bound mCLICK-III was detected by Western blot with an anti-HA tag monoclonal antibody (1:2500, 12CA5; Roche Diagnostics).

Immunoprecipitate Kinase Assay—COS-7 cells were plated onto 6-well plates at a density of 2 × 10^5 per well, and 12 h later were transiently transfected with pcDNA3-HAmCL3wt (0.3 μg), pcDNA3-HAmCL3dC (0.3 μg), or empty vector (0.3 μg) and pd2EGFPN1-CaMKKactiveMyc (0.6 μg), or empty vector (0.6 μg) using LipofectAMINE 2000 reagent. For immunoprecipitate kinase assay, cells were washed twice with ice-cold PBS(−) and lysed in lysis buffer containing 20 mM Tris-HCl (pH 8.0), 100 mM NaCl, 5 mM $MgCl_2$, 1% Nonidet P-40, 1 mM dithiothreitol, 25 mM NaF, 10 mM β-glycerophosphate, 5 mM sodium pyrophosphate, 0.1 μM calyculin A, and protease inhibitors. Lysates were immunoprecipitated with an anti-HA antibody (12CA5) and protein-G-Sepharose (Amersham Biosciences). Immunoprecipitates were washed three times in the lysis buffer and washed twice in kinase buffer containing 50 mM HEPES-NaOH (pH 7.5), 10 mM $MgCl_2$, 1 mM Ca^{2+}, 20 mM β-glycerophosphate, 0.02% Nonidet P-40, 1 mM dithiothreitol, and protease inhibitors. Kinase assay was performed in the presence of 1 μM CaM, 50 μM ATP, 0.5 μCi of [γ-^{32}P]ATP in the kinase buffer using 2.5 μg of CREM (cAMP-response element modulator) (Santa Cruz Biotechnology) or 5 μg of MBP (Calbiochem) as substrates for 10 min at 30 °C. For kinase assay without Ca^{2+}/CaM, 1 μM CaM was omitted, and 1 mM EGTA was substituted for 1 mM Ca^{2+} in the kinase buffer.

Luciferase Assay—COS-7 cells were plated onto 24-well plates at a density of 5 × 10^4 per well, and 12 h later were transfected with pFR-Luc, pFA-CREB, pRL-CMV (200 ng, 50 ng, 4 ng each; Stratagene), and pIRES-HAmCL3dC (100 ng). 24 h after transfection, luciferase

[2] S. Ohmae, S. Takemoto-Kimura, and H. Bito, manuscript in preparation.

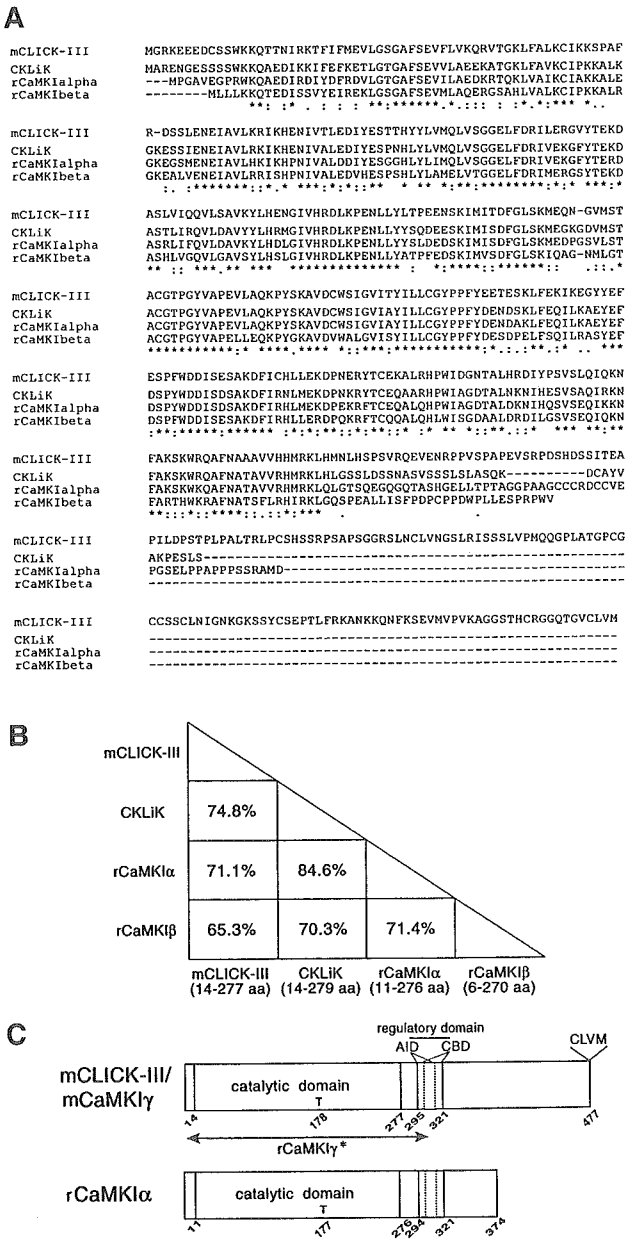

FIG. 1. **CLICK-III/CaMKIγ is an isoform of the CaMKI family with an unusually extended C-terminal domain.** *A*, the deduced amino acid sequence of mCLICK-III was aligned with CKLiK, rCaMKIα, and rCaMKIβ by using the ClustalW Multiple Sequence Alignment Program version 1.8. The *asterisks* indicate positions of identical amino acid residues. The *colons* and *dots* indicate stronger and weaker degrees of residue conservation, respectively. *B*, comparison of amino acid identities between kinase domain sequences of known CaMKI-related kinases. The kinase domain of mCLICK-III shows high identity with all known CaMKI-related kinases, CKLiK (74.8%), CaMKIα (71.1%), and rCaMKIβ (65.3%), respectively, in the order of identity (*left column*). The exact position of amino acid (*aa*) residues used for comparison are shown in *parentheses*. *C*, similarity and difference between CLICK-III and other CaMKI-related kinases. CLICK-III shares a high homology in its catalytic domain at the N terminus followed by a regulatory domain consisting of an autoinhibitory domain (*AID*) and a Ca^{2+}/CaM binding domain (*CBD*). Unlike the other CaMKI-related kinases, however, mCLICK-III has a distinctively longer C-terminal region ending with a putative *CAAX* motif (*CLVM*). A 309-amino acid-long partial sequence of rat of CLICK-III has been reported before as a rat CaMKIγ (*asterisk*) (19). GenBank™ accession numbers are as follows: mCLICK-III, AY212936; CKLiK, AF286366; rCaMKIα, L24907 and L26288; rCaMKIβ, D86556; and rCaMKIγ (partial cDNA), D86557.

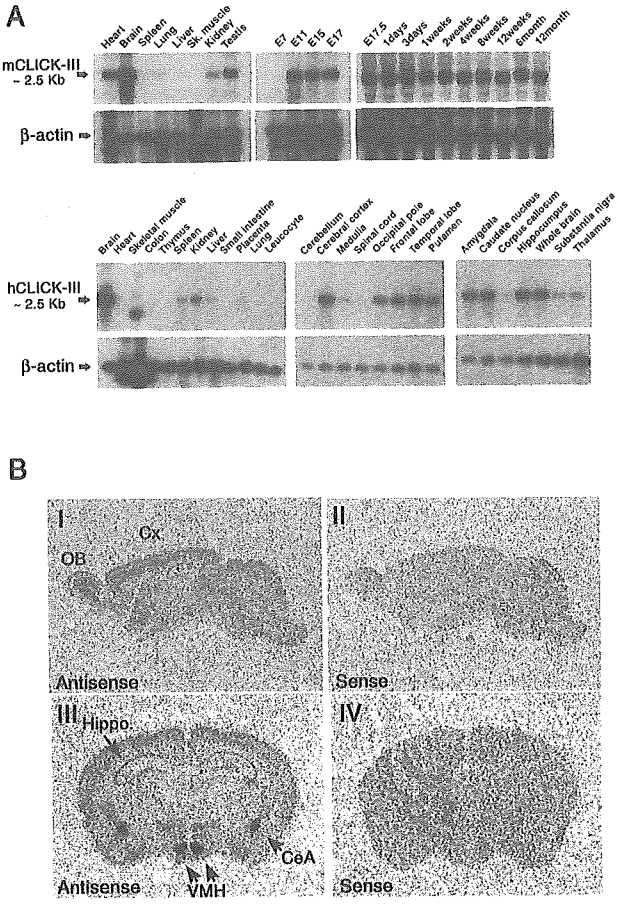

FIG. 2. **Abundant expression of CLICK-III transcripts in the CNS.** *A*, Northern blotting using specific probes for CLICK-III showed that both mCLICK-III and hCLICK-III are most strongly expressed in the brain. Note that mCLICK-III transcripts are expressed from embryonic day (*E*) 11, and hCLICK-III transcripts are expressed in a forebrain-specific manner in the CNS. *Sk*, skeletal. *B*, *in situ* hybridization was performed with ^{35}S-labeled riboprobes. Film autoradiographs of mouse brain parasagittal (*I* and *II*) and coronal sections (*III* and *IV*) showed specific hybridization signals for mCLICK-III antisense probes in restricted brain areas such as the olfactory bulbs (*OB*), the cerebral cortex (*Cx*), the hippocampus (*Hippo.*), the central nucleus of amygdala (*CeA*), and the ventromedial nucleus of hypothalamus (*VMH*). These signals disappeared when sense probes were used (*II* and *IV*).

activity was measured using Dual-Luciferase Reporter Assay System (Promega) according to the manufacturer's protocol. The firefly and the *Renilla* luciferase activities were both measured using SIRIUS luminometer (Berthold). All results were normalized using *Renilla* luciferase (pRL-CMV), which was co-transfected with the other reporter genes (pFR-Luc and pFA-CREB).

Culture and Transient Transfection of CA1/CA3 Hippocampal Neurons—Culture of mouse CA1/CA3 hippocampal neurons was carried out as described previously for rat (16). A cDNA transfection was carried out at 7 days *in vitro* using a modification of the calcium phosphate method.[3]

BODIPY-TR-ceramide Labeling and Fluorescence Microscopy—For BODIPY-TR-ceramide (Molecular Probes) and green fluorescent protein (GFP) imaging, COS-7 were plated on Lab-Tek chambered coverglass (4 well, Nunc) and transfected with expression vectors (0.4 μg/well), pEGFP-rCaMKIα, pEGFP-mCL3, pEGFP-mCL3C474S, and pEGFP-CLVM using LipofectAMINE 2000 reagent. After 24 h, the cells were rinsed twice in HBSS/HEPES, incubated for 20 min at room temperature with 2.5 μM BODIPY-TR ceramide/bovine serum albumin in HBSS/HEPES. The cells were washed twice with HBSS/HEPES and replaced with pre-warmed fresh medium, followed by a 1-h incubation

[3] S. Takemoto-Kimura and H. Bito, manuscript in preparation.

in a CO_2 incubator. To simultaneously acquire GFP and BODIPY-TR-ceramide images under live conditions, a Carl Zeiss LSM 510 system equipped with a Carl Zeiss Axiovert 100TV inverted microscope and a ×63 Plan-Apochromat (NA 1.4, oil) objective (Carl Zeiss) was used. For all images, stacks of multiple Z-scan sections were obtained, and projected images were calculated off-line using a projection software on the LSM 510 system. All pseudocolor representations were assembled using Photoshop version 5.5 (Adobe). For compactin pretreatment, the normal medium was replaced with a growth medium containing 40 μM compactin (Wako Pure Chemicals) for 12 h. No apparent phototoxicity was observed under our experimental conditions.

Subcellular Fractionation—COS-7 cells were grown to 70% confluency on a 10 cm-dish and transfected with each expression vector (4 μg per dish) using LipofectAMINE 2000 reagent. 48 h after transfection, the cells were washed twice in ice-cold PBS(−), suspended in 250 μl (per dish) of homogenizing buffer containing 10 mM HEPES-NaOH (pH 7.5), 10 mM KCl, 2 mM $MgCl_2$, protease inhibitors, disrupted in a Potter-Elvehjem homogenizer with 40 strokes, and adjusted to 0.25 M sucrose. To remove unbroken cells and nuclei, the homogenate was centrifuged at 600 × *g* for 10 min. The supernatant was separated by centrifugation at 100,000 × *g* for 60 min. After collecting the resulting supernatant (cytosolic fraction, S), the membrane pellet was washed once in the homogenizing buffer containing 0.25 M sucrose and again centrifuged at 100,000 × *g* for 60 min. For the salt wash experiment, the 600 × *g* supernatant was divided into two microtubes and separated by ultracentrifugation at 100,000 × *g* for 60 min. The membrane pellet was resuspended in homogenization buffer containing 10 mM HEPES-NaOH (pH 7.5), 10 mM KCl, 2 mM $MgCl_2$, 0.25 M sucrose or high salt homogenization buffer containing 1 M NaCl, followed by incubation on ice for 1 h, and ultracentrifuged again at 100,000 × *g*. For all analyses, the membrane pellets were finally extracted with the elution buffer containing 25 mM HEPES-NaOH (pH 7.5), 2% SDS, 150 mM NaCl, protease inhibitors for 1 h at room temperature and centrifuged for 15 min at 15,000 rpm. This supernatant was collected and designated as crude membrane fraction (P or P′). The volume of the elution buffer was adjusted to be equal to the volume of input (identical to the 600 × *g* supernatant). For Western blot analyses, one-third volume of 4× Laemmli buffer was added and boiled for 4 min, and 20 μl of each fractions were subjected to SDS-PAGE. For compactin treatment, the medium was replaced with growth medium containing 40 μM compactin for 16 h.

Western Blot Analysis—After SDS-PAGE, the proteins were transferred onto a nitrocellulose membrane (Optitran BAS-85, Schleicher & Schuell), and immunoreactive proteins were detected using ECL-Plus (Amersham Biosciences) with the following concentration of primary antibodies: anti-HA tag monoclonal antibody (1:2500, 12CA5; Roche Applied Science), anti-GFP monoclonal antibody (1:1000, 3E6; Molecular Probes), and anti-phospho-CREB (Ser-133) polyclonal antibody (1:1000; Cell Signaling). Horseradish peroxidase-linked anti-mouse or anti-rabbit IgG (1:2000; Amersham Biosciences) were used as secondary antibodies. The chemiluminescence image was acquired using a FAS-1000 system (Toyobo) equipped with a 16-bit cooled CCD camera. For quantification of signal intensity of detected immunoreactive bands, a rectangular window, which had a sufficient area to completely surround each band, was defined, and the total pixel intensity of each area was calculated using Photoshop 6.0 (Adobe). The signal intensity was normalized as a percentage of the total intensity, calculated as the sum of the band intensities detected in cytosolic and membrane fractions (S or P or P′/(S + P)). Statistical analyses were carried out using Prism 3.0 (GraphPad software). Statistical significance ($p < 0.05$) was determined between two groups using unpaired Student's *t* test and between three groups using one-way analysis of variance (followed by post hoc Bonferroni and Neuman-Keuls tests). All data are given as means ± S.E.

RESULTS

Molecular Cloning of CLICK-III, a Novel Brain-enriched CaMK—During the course of studying two novel putative CaMK-like CREB kinase-I and -II (CLICK-I and -II) cloned by degenerate PCR strategies,[2] BLAST search revealed the presence of a putative human gene product with high homology to both CLICKs. We named this novel kinase human CLICK-III. A putative open reading frame of human CLICK-III had been deposited as a novel rat Ca^{2+}/calmodulin-dependent protein kinase-like gene, an assembly of presumed exon sequences obtained from the draft Human Genome Sequence (GenBank™ accession number AL023754). We cloned a human CLICK-III (hCLICK-III) cDNA (GenBank™ accession number AY212935) by PCR from a human hippocampal cDNA pool, using primer sequences corresponding to the deposited sequence, and we confirmed the authenticity of this gene product. We next used a 3′-RACE strategy to obtain a full-length mouse hippocampal CLICK-III cDNA (GenBank™ accession number AY212936). Mouse CLICK-III (mCLICK-III) showed a high degree of amino acid identities with CKLiK, a recently reported CaMK-like kinase (18), as well as with rat CaMKIα (13) and CaMKIβ (19) (Fig. 1, *A* and *B*). A partial sequence of a rat ortholog of CLICK-III was previously reported as rCaMKIγ (19) (*asterisk*, Fig. 1*C*).

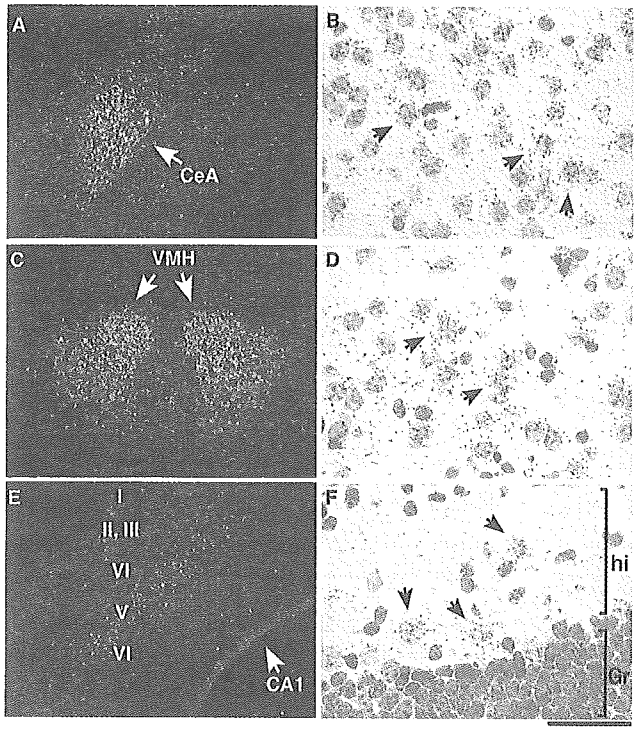

FIG. 3. **CLICK-III transcripts are expressed in neurons.** Dark- (*A*, *C*, and *E*) and bright-field (*B*, *D*, and *F*) photomicrographs showed strong signals in the central nucleus of amygdala (*A*, *CeA*) and the ventromedial hypothalamic nucleus (*C*, *VMH*) (also see Fig. 2*B*, *III*). Silver grains were present only on neuronal cell bodies (*arrows*, *B* and *D*). Moderate signals were detected on the layer *V* pyramidal neurons in the cerebral cortex and the *CA1* pyramidal neurons in the hippocampus (*E*). In the hippocampus, non-principal neurons were also labeled with silver grains (*arrows*, *F*). *CA1*, CA1 area for Ammon's horn; *hi*, the hilus of the dentate gyrus; *Gr*, the granule cell layer of the dentate gyrus. *Scale bars*, *A*, *C*, and *E*, 0.5 mm; *B*, *D*, and *F*, 50 μm.

The open reading frame of CLICK-III cDNAs contained an N-terminal kinase domain, a conserved threonine at position 178 in the activation loop, and an overlapping autoinhibitory/Ca^{2+}/CaM-binding domain in its middle portion; these domains showed high homology across the CaMKI-related kinases (Fig. 1*B*). The C-terminal end of CLICK-III was unusually extended in comparison with CKLiK, CaMKIα, and CaMKIβ, suggesting a unique role for CLICK-III (Fig. 1*C*). The very C-terminal end of hCLICK-III and mCLICK-III were, however, divergent, indicating the existence of multiple C-terminal variants (data not shown).

As shown in Fig. 2*A*, Northern blot analyses suggested that in adult tissues, mCLICK-III was highly expressed in the brain, although heart, testis, and kidney also showed detectable amounts of hybridization signals. The mCLICK-III transcript first became detected at embryonic day 11 (E11), in parallel with the onset of the development of the central nervous system (CNS). Its expression level remained constant from E11 onward, throughout development and during adulthood

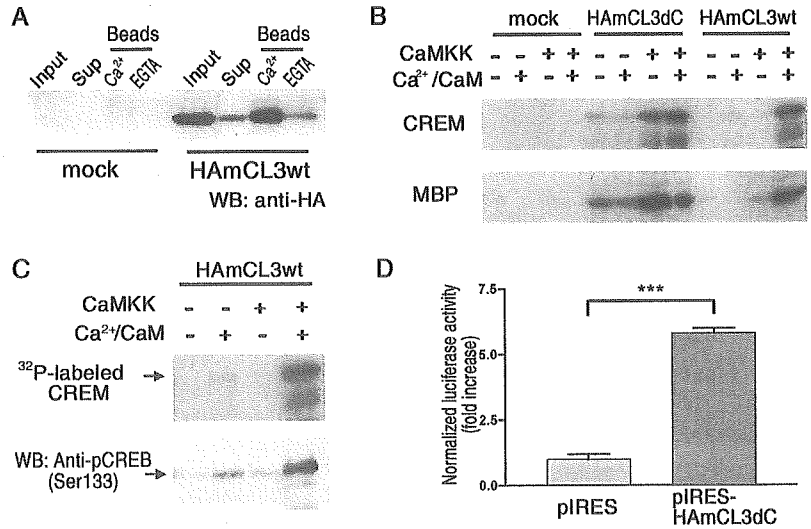

FIG. 4. **Activation of CLICK-III by Ca^{2+}/CaM and CaMKK.** *A*, mCLICK-III expressed in COS-7 cells is bound to CaM-Sepharose beads in the presence of Ca^{2+}. Lysates from COS-7 cells transfected with either an empty vector (*mock*) or a mCLICK-III cDNA (*HAmCL3wt*) were incubated with CaM-Sepharose beads. mCLICK-III remained bound to CaM-Sepharose after washing in the presence of 2 mM Ca^{2+} (*Beads, Ca^{2+}*), whereas most CLICK-III was washed out in 0 mM Ca^{2+}, 2 mM EGTA (*Beads, EGTA*). *WB*, Western blot. *B*, immunoprecipitate kinase assays of CLICK-III. COS-7 cells were transfected with an empty vector (*mock*), a wild type mCLICK-III cDNA (*HAmCL3wt*), or mCLICK-III C-terminal deletion mutant (*HAmCL3dC*) with (+) or without (−) a cDNA encoding a constitutive active form of rat CaMKKα (*CaMKK*). After immunoprecipitation with an anti-HA antibody, kinase assays were performed in the presence (+) or the absence (−) of Ca^{2+}/CaM using MBP (5 μg) or CREM (2.5 μg) as substrates. Note that both mCL3wt and mCL3dC require CaMKK activity for their full activation. C-terminal deletion mutant of mCLICK-III showed a clear constitutive kinase activity in the presence of CaMKK, independent of the presence of Ca^{2+}/CaM, whereas the wild type kinase was only active in the presence of Ca^{2+}/CaM. *C*, CREM phosphorylation was also detected in a manner similar to ^{32}P incorporation, using an anti-phospho-CREB (Ser-133) antibody. *D*, the C-terminal deletion mutant of CLICK-III can activate CREB-dependent transcription in COS-7. Cells were transfected with CLICK-III C-terminal deletion mutant (*pIRES-HAmCL3dC*) and reporter genes coding Gal4-CREB and UAS-luciferase and collected, and lysates were extracted to measure the luciferase activity 24 h later. The *bars* represent luciferase activities relative to that of mock-transfected lysates (*pIRES*) and are shown as means ± S.E. (n = 3). *** denotes $p < 0.001$.

(Fig. 2*A*, *upper panels*). In human mRNA blots, CLICK-III expression was almost confined to the brain, with small amount of signals in the skeletal muscles, kidney, spleen, and liver (Fig. 2*A*, *lower panels*). Within the CNS, the strongest signal was detected in the forebrain neocortex (cerebral cortex, occipital pole, frontal lobe, and temporal lobe), the striatum (putamen and caudate nucleus), and the limbic system (amygdala and hippocampus) (Fig. 2*A*, *lower panels*).

CLICK-III Is Neuronally Expressed and Is Abundant in the CeA and the VMH—We next examined CNS expression of CLICK-III mRNA by *in situ* hybridization using ^{35}S-labeled cRNA riboprobes. X-ray film autoradiography of hybridized parasagittal and coronal sections showed specific signals in the neuronal cell layers of the cerebral cortex, olfactory bulb, and hippocampus (Fig. 2*B*, *I* and *III*). Most remarkably, intense hybridization signals were shown in the CeA and the VMH (Fig. 2*B*, *III*). We obtained identical results using two independent antisense probes, either from the N-terminal or from C-terminal regions (data not shown), whereas sense probes only generated background signals (Fig. 2*B*, *II* and *IV*). Hybridization in the presence of excess cold riboprobes also completely abolished the antisense probe signals (data not shown), confirming the specificity of these obtained signals.

Emulsion autoradiography of individual sections revealed that CLICK-III was particularly expressed in neurons, but not found in glia, in any areas that we examined. Heavy amounts of silver grains associated with most neuronal cell bodies present in the CeA (Fig. 3, *A* and *B*) and the VMH (Fig. 3, *C* and *D*). Pyramidal cells in the cerebral cortex, especially in the layer V, and those in the area CA1 of the hippocampus were also positive in CLICK-III mRNA signals (Fig. 3*E*). In contrast, in the dentate gyrus of the hippocampus, only scattered non-principal cells, presumably hilar interneurons, had significant amount of silver grains (Fig. 3*F*).

Taken together, these sets of data established that CLICK-III was a CaMKI family member specifically expressed in neurons, with a remarkable abundance in the CeA and VMH. Such specificity in its expression profile particularly stands out

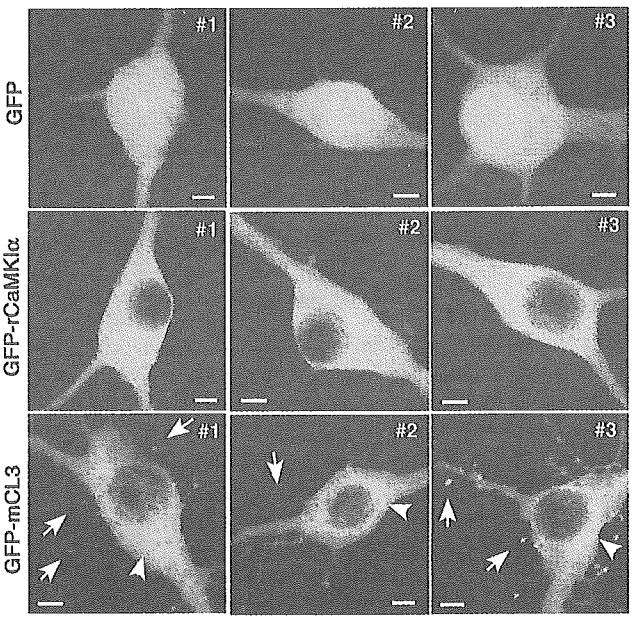

FIG. 5. **GFP-rCaMKIα and GFP-mCL3 show distinct subcellular localization in hippocampal neurons.** Mouse CA1/CA3 hippocampal neurons were transfected with GFP, GFP-rCaMKIα, and GFP-mCL3 for 7 days *in vitro*, fixed 48 h later, and examined by confocal microscopy. Three representative neurons were shown for each construct (*#1–#3*). GFP showed diffuse distribution across the cell, whereas GFP-rCaMKIα was diffusely expressed mainly in the cytoplasm. In contrast, GFP-mCL3 expression was more localized in specific intracellular compartments (*arrowheads*) and concentrated at the tips of filopodia-like processes (*arrows*). *Bar*, 5 μm.

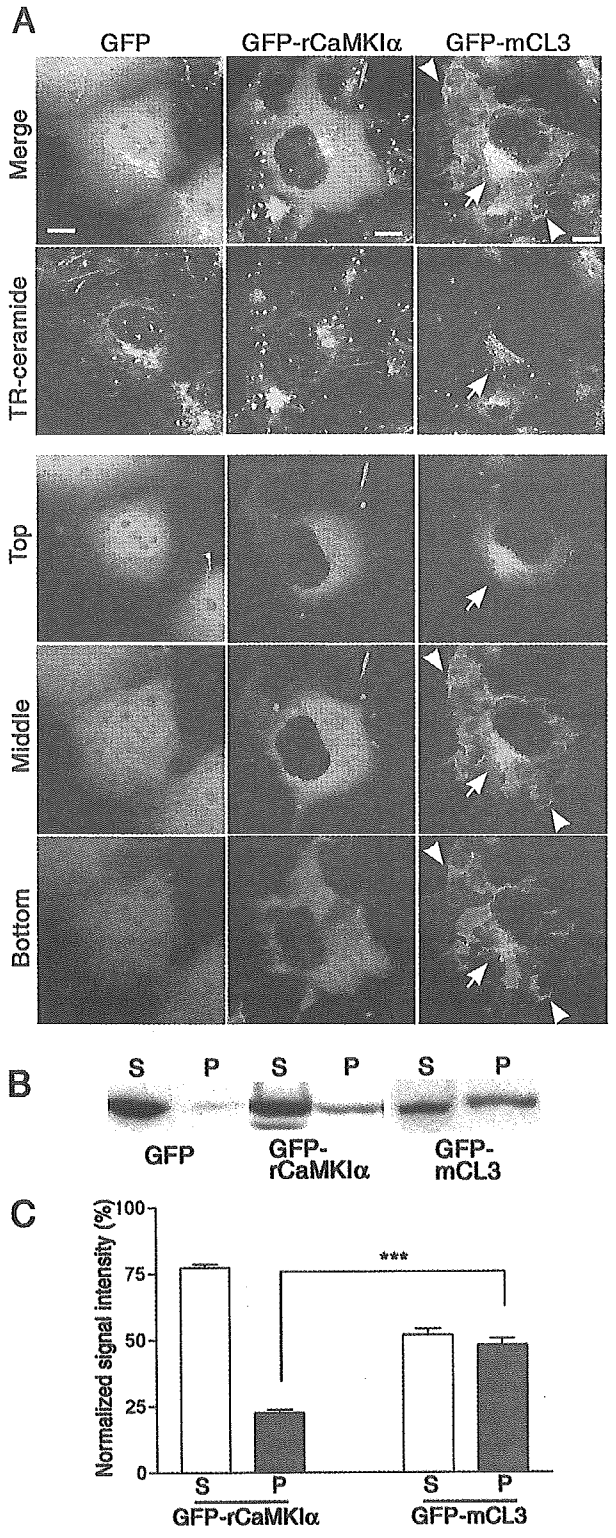

FIG. 6. **Localization of GFP-mCL3 with the Golgi complex and plasma membranes in COS-7 cells.** *A*, COS-7 cells transfected with GFP, GFP-rCaMKIα, and GFP-mCL3 were stained with a Golgi-specific vital dye (BODIPY TR-ceramide) and examined under live conditions. Projected images from stacks of z-planes (*Merge* and *TR-ceramide*) and single z-plane images taken near the *bottom*, *middle*, and *top* of the cells showed localization of CLICK-III to the Golgi complex (*arrows*) and to the plasma membranes (*arrowheads*). *Green*, GFP image; *red*, BODIPY TR-ceramide. *Bar*, 10 μm. *B*, lysates of COS-7 cells transfected with the indicated constructs were fractionated by ultracentrifugation at 100,000 × *g*. The supernatants (*S*) were collected as cytosolic fractions, and the pellets (*P*) were washed once and centrifuged again. The resulting pellet was recovered as crude membrane fraction (*P*). Each fraction was blotted and visualized using an anti-GFP antibody. *C*, chemiluminescent signal intensities, quantified by a CCD camera-based imaging system, were presented in percentages relative to the total signal intensities detected in both fractions (*S* + *P*). The *bars* represent means ± S.E. ($n = 4$). ***, $p < 0.001$.

TABLE I
C-terminal sequences of Ras proteins and mCLICK-III
CAAX motifs are shaded with a gray box.

mCLICK-III	GSTHCRGGQTGVCLVM
H-ras	PDESGPGCMSCKCVLS
N-ras	SDDGTQGCMGLPCVVM
K-ras(4B)	DGKKKKKKSKTKCVIM

among all CaMKs presently identified (16–21, 35–37).

Enzymatic Properties of CLICK-III—We next tested whether CLICK-III was indeed a Ca^{2+}/CaM-dependent protein kinase, as suggested from its domain structure (Fig. 1*B*). To this end, an HA-tagged CLICK-III was constructed and transfected to COS-7 cells. Crude lysates of transfected COS-7 cells were collected and incubated with CaM-Sepharose beads in the presence of 2 mM Ca^{2+}. The beads were centrifuged and separated from the supernatant and then washed several times in the presence or absence of Ca^{2+}. SDS-PAGE analyses showed that HA-immunoreactive bands were mostly recovered with the beads in the presence of Ca^{2+}, whereas they were largely washed out in 0 Ca^{2+}, 2 EGTA (Fig. 4*A*). Thus, CLICK-III was clearly able to bind CaM in a Ca^{2+}-dependent manner.

Ca^{2+}/CaM-dependent regulation of the protein kinase activity of CLICK-III was investigated using an immunoprecipitate kinase assay, with MBP and CREM as kinase substrates (Fig. 4*B*). Both Ca^{2+}/CaM and CaMKK cotransfection were required to reach maximal levels of activation of the wild type CLICK-III (HAmCL3wt). In contrast, a C-terminal deletion mutant in which the entire autoinhibitory/Ca^{2+}/CaM binding domain was removed (HAmCL3dC) showed a constitutive, Ca^{2+}-independent kinase activity even in the absence of Ca^{2+}, when active CaMKK was cotransfected (Fig. 4*B*). CLICK-III activity monitored with [γ-^{32}P]ATP incorporation into CREM closely paralleled the amount of phospho-CREB Ser-133 immunoreactivity, suggesting that wild type CLICK-III is able to directly phosphorylate CREB at Ser-133, in a Ca^{2+}/CaM- and CaMKK-dependent manner, at least *in vitro* (Fig. 4*C*). We further confirmed that CLICK-III may work as CREB kinase *in vivo* by using a Gal4-CREB/UAS-luciferase reporter system. Transfection of a constitutively active CLICK-III (pIRES-HAmCL3dC) significantly augmented CREB-dependent gene expression in COS-7 cells (Fig. 4*D*). The result was normalized using *Renilla* luciferase (pRL-CMV), which was co-transfected with the other reporter genes (pFR-Luc and pFA-CREB).

Taken together, these data indicated that the enzymatic properties of CLICK-III recapitulated all major features of CaMKI isoforms, such as dual regulation by Ca^{2+}/CaM and CaMKK, and activation of CREB pathway *in vitro* and in a heterologous system.

Membrane Localization of CLICK-III in Hippocampal Neurons and in COS-7 Cells—As we failed to raise high titer antibodies against CLICK-III, we expressed GFP-tagged CLICK-III in hippocampal pyramidal neurons 7 days *in vitro*, and we monitored its subcellular distribution in fixed (Fig. 5) or live samples (data not shown). Under either condition, GFP alone was diffusely distributed throughout the cytoplasm and the nucleus, whereas GFP-rCaMKIα remained largely ex-

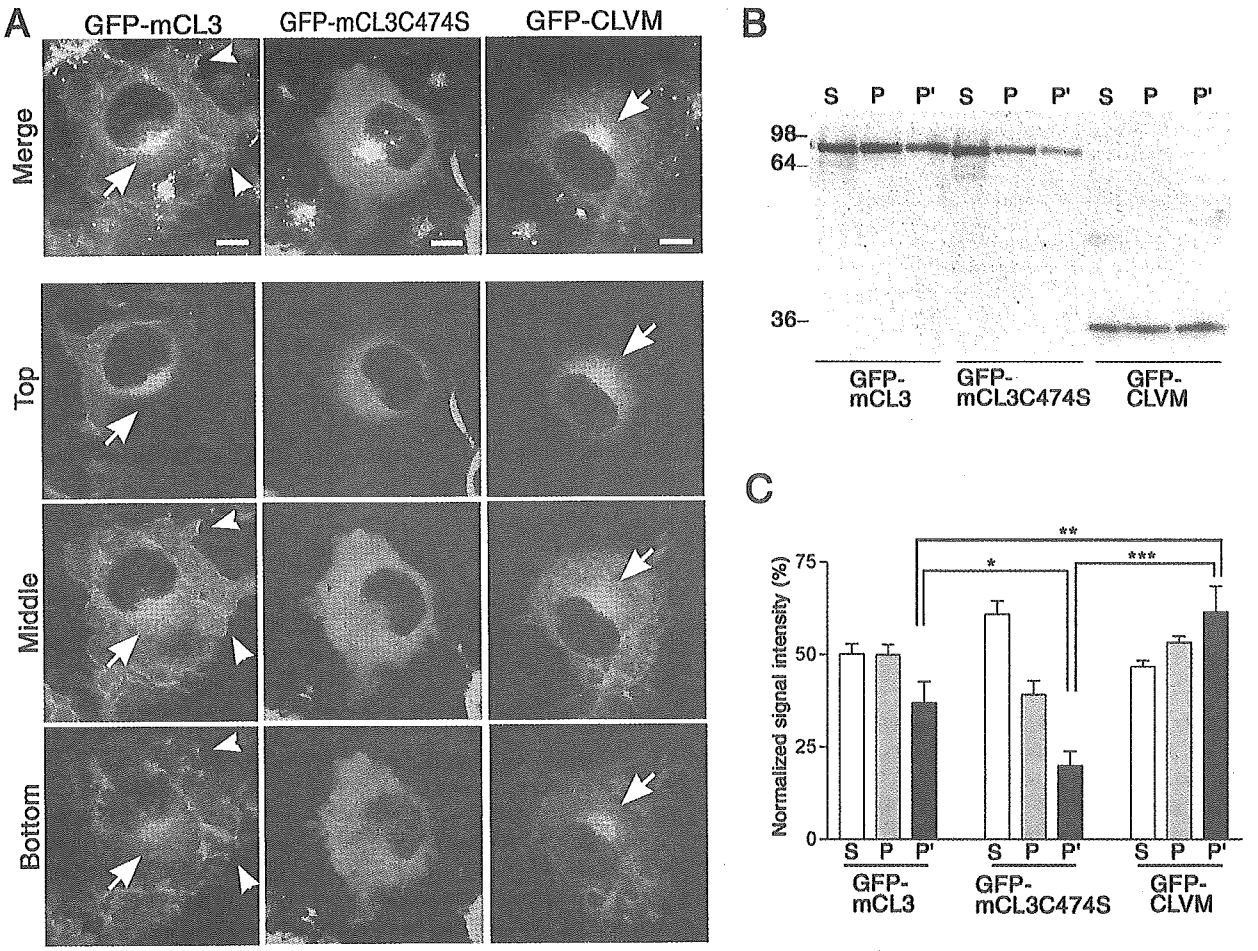

FIG. 7. **A critical role of the C-terminal *CAAX* motif in determining mCLICK-III localization.** *A*, COS-7 cells transfected with either wild type CLICK-III (*GFP-mCL3*), a mutant that has a point mutation at the prenylation site of *CAAX* motif (*GFP-mCL3C474S*), or *GFP-CLVM* were stained with BODIPY TR-ceramide and examined alive. The *arrows* and *arrowheads* indicate the localization to the Golgi complex and to the plasma membranes, respectively. *Merge*, projected images; *top*, *middle*, and *bottom*, single *z*-plane images. *Green*, GFP image; *red*, BODIPY TR-ceramide. *Bar*, 10 μm. *B*, COS-7 lysates were fractionated by ultracentrifugation at 100,000 × *g*. The supernatants were collected (*S*), and the pellets (*P*) were washed in either normal homogenization buffer or high salt homogenization buffer, followed by ultracentrifugation at 100,000 × *g*. The cytosolic fractions (*S*), the membrane fractions (*P*), and the high salt-washed membrane fractions (*P'*) were subjected to Western blotting with an anti-GFP antibody. *C*, quantification of signal intensities detected in *B*. The *bars* represent means ± S.E. (wt, $n = 4$; C474S, $n = 4$; CLVM, $n = 3$). *, $p < 0.05$; **, $p < 0.01$; ***, $p < 0.001$.

cluded from the nucleus, in keeping with prior reports (Fig. 5) (15, 16). A striking difference was noted in the subcellular localization of GFP-tagged CLICK-III (GFP-mCL3); GFP-mCL3 distribution was not diffuse but seemed rather associated with intracellular compartments reminiscent of endomembrane systems such as the Golgi complexes or the endoplasmic reticulum (Fig. 5, *arrowheads*). Furthermore, CLICK-III was also found to be enriched at the tips of thin processes that were most likely filopodia (Fig. 5, *arrows*); these structures have been proposed to constitute intermediate membrane protrusions that precede the formation of stable dendritic spines during synaptogenesis (38).

To better analyze in detail the potential mechanisms that might underlie the distinct localization of CLICK-III, we overexpressed CLICK-III in COS-7 cells. Ectopic expression of GFP-mCL3 in COS-7 cells confirmed that subcellular distribution of CLICK-III was indeed distinct from that of GFP or GFP-rCaMKIα. Unlike the diffuse distribution of GFP (Fig. 6*A*, *left panels*) or the largely cytoplasmic distribution GFP-rCaMKIα (Fig. 6*A*, *middle panels*), GFP-mCL3 localization overlapped with the perinuclear Golgi complex, as demonstrated by a high degree of spatial superimposition between GFP fluorescence of GFP-mCL3 and a Golgi-specific vital dye, BODIPY TR-ceramide (Fig. 6*A*, *right panels*, *arrows*). Such a co-localization was not detected between GFP-rCaMKIα, or GFP alone, and the BODIPY TR-ceramide stain (Fig. 6*A*, *upper panels*). In addition, a significant amount of GFP-mCL3 signals was seen at the plasma membranes (Fig. 6*A*, *right panels*, *arrowheads*). Consistent with such significant localization of GFP-mCL3 with the Golgi complex and the plasma membranes, a sizable pool of GFP-mCL3 protein was recovered in the membranes fraction (P), after 100,000 × *g* ultracentrifugation (Fig. 6, *B* and *C*). In contrast, GFP-rCaMKIα was predominantly present in the supernatants (S) and little in the membrane pellet fraction (P) (Fig. 6, *B* and *C*).

A Critical Role for a CAAX Motif in the Localization of CLICK-III to the Golgi Complex and Plasma Membranes—What might be the cause of such distinct subcellular localization between rCaMKIα and CLICK-III? Sequence search identified a putative *CAAX* membrane-anchoring motif in the very C-terminal end of mCLICK-III (Fig. 1 and Table I). We thus examined whether the *CAAX* box in mCLICK-III was necessary for its membrane localization. A single amino acid substitution at the putative prenylation site (GFP-mCL3C474S) completely abolished recruitment of mCL3 to the perinuclear Golgi (Fig. 7*A*, *left panels*, *arrows*) and plasma membranes (Fig. 7*A*,

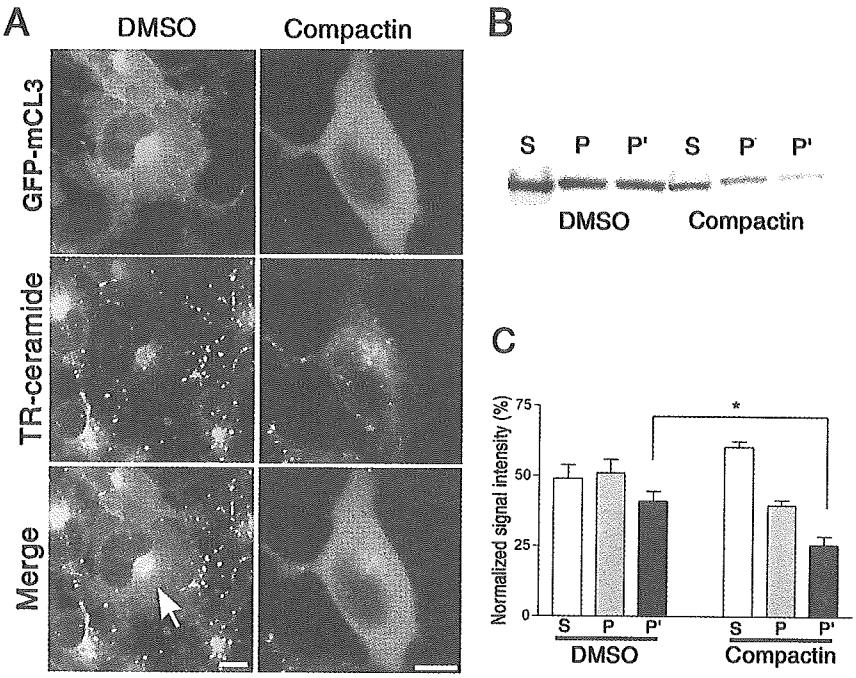

FIG. 8. **Compactin, an HMG-CoA reductase inhibitor, prevents GFP-mCL3 localization to the Golgi and plasma membranes.** *A*, COS-7 cells transfected with GFP-mCL3 were pretreated with vehicle alone (*DMSO*) or 40 μM compactin for 12 h, stained with BODIPY TR-ceramide, and examined under live conditions. The co-localization of GFP-mCL3 and BODIPY TR-ceramide (*arrow*) was abolished in compactin-treated cells. *Green*, GFP image; *red*, BODIPY TR-ceramide. *Bar*, 10 μm. *B*, COS-7 cells transfected with GFP-mCL3 were treated with 40 μM compactin for 16 h. The cytosolic fractions (*S*), the membrane fractions (*P*), the high salt-washed membrane fractions (*P'*) were collected and subjected to Western blotting using an anti-GFP antibody. *C*, quantification of signal intensities detected in *B*. The *bars* represent means ± S.E. (n = 5). * denotes $p < 0.05$.

left panels, arrowheads), and this mutant was now diffusely expressed in the cytoplasm (Fig. 7*A*, *middle panels*). Conversely, attachment of the *CAAX* box (CVLM) of the mCL3 to the C terminus of GFP (GFP-CLVM) was sufficient to confer perinuclear Golgi localization to GFP (Fig. 7*A*, *right panels*, *arrows*). We found, however, that GFP-CLVM did not appear to localize well to the plasma membranes, consistent with the notion that residues upstream of the *CAAX* motif may also play a role in the correct localization and the proper sorting to the plasma membranes (Fig. 7*A*, *right panels*) (22, 23). In accordance with these observations, biochemical fractionation experiments showed a significant reduction in the amount of membrane-bound GFP-mCL3C474S especially after high salt wash (P'), whereas GFP-CVLM still remained heavily associated with the membranes (Fig. 7, *B* and *C*). Together, these data suggested that the *CAAX* box of CLICK-III is necessary to localize CLICK-III to the Golgi membranes.

To confirm this point further, mCL3-overexpressing cells were pretreated with compactin, an HMG-CoA reductase inhibitor. As blockade of this rate-limiting step of cholesterol synthesis should also significantly reduce prenylation of the *CAAX* box cysteine (33), we expected that compactin treatment should mimic the effect of Cys-to-Ser mutation at position 474. Consistently, although vehicle (Me_2SO) treatment had no effect on localization of GFP-mCL3, which was strongly detected in association with Golgi and plasma membranes (Fig. 8*A*, *left panels*, *arrow*), an overnight compactin treatment dramatically abolished this membrane anchoring (Fig. 8*A*, *right panels*). Prevention of membrane recruitment of GFP-mCL3 and its retention to the soluble fractions by compactin treatment was also verified by using biochemical fractionation as well (Fig. 8, *B* and *C*).

Together, these experiments demonstrated that CLICK-III, a neuronally expressed CaMKI isoform, was able to be localized to the Golgi apparatus and plasma membranes, at least in part, via its C-terminal *CAAX* box in a prenylation-dependent manner.

DISCUSSION

CaMK represents a class of the multifunctional protein kinase family, with a particular significance for the physiology of excitable cells such as neurons or smooth muscles (1–10). A better understanding of the role of neuronal CaMKs has been of urgency because CaMK activity has been suggested to be crucial for linking neuronal activity with various types of neuronal plasticity (2–4, 8–11, 39–42). Recent experiments have further revealed that, in fact, various CaMK isoforms play a critical role in establishing distinct types of memory in mammals (9, 12, 43–46). So far, however, most analyses have focused on the role of CaMKIIα, β, and CaMKIV, because these are the most well characterized CaMKs widely expressed in forebrain neurons (35, 36). In contrast, studies concerning CaMKI have lagged behind, in part because the originally isolated CaMKIα has been expressed ubiquitously and little has been shown so far about its physiological role or substrates in neurons (13, 15, 17).

In this study, we have identified a neuronally enriched CaMKI isoform that has the potential to be membrane-anchored. This CaMKI isoform, CLICK-III/CaMKIγ, possessed an extended C-terminal domain distinct from known CaMKs. We found that CLICK-III had three particular characteristics that were noteworthy.

First, we confirmed that the activation of CLICK-III required not only Ca^{2+}/CaM but also a phosphorylation by other kinases, presumably by a CaMKK. Such strong CaMKK dependence for its enzymatic activation was qualitatively similar to what was reported previously for CaMKIα (27–29), indicating that the catalytic core of CLICK-III may resemble CaMKIα and may be regulated in a manner identical to CaMKIα. Thus, maximal activation of CLICK-III might only be triggered in close vicinity to an upstream kinase such as CaMKK.

Second, unlike CaMKIα, however, CLICK-III expression was strongly enriched in neurons. More interestingly, examination of its mRNA distribution, by *in situ* hybridization analyses, revealed a very strong expression in the CeA and the VMH. Such peculiar distribution stands out among all known CaMKs and indicates the possibility that CLICK-III may play a role in the proper function of these nuclei. The CeA has been shown to be a relay for most autonomic outputs and, furthermore, has been associated with the expression of the stimulus-specific state of fear (47). The VMH, on the other hand, has been linked

with control of the homeostasis of feeding and sexual behaviors (48, 49). Future studies are needed to determine whether some of these functions mediated through either CeA or VMH might indeed be controlled by the kinase activity of CLICK-III.

Third, our studies have clarified for the first time a mechanism by which CaMK may be anchored to the Golgi and plasma membranes. A *CAAX* motif that we identified in the unusually extended C-terminal end of CLICK-III played a critical role in determining the targeting of CLICK-III to the membrane compartments in a heterologous expression system. The high degree of sequence similarity of the *CAAX* motif of CLICK-III with that of Ras (Table I) and the disruption of membrane anchoring by either a point mutation at the putative prenylation site or by pretreatment with an HMG-CoA reductase inhibitor have suggested that prenylation of the *CAAX* box may constitute a mechanism through which CLICK-III may be actively sorted to the membranes. The prenyl moiety is derived from the mevalonate/cholesterol biosynthetic pathway. It is interesting to note that this pathway has been shown recently (50, 51) to affect various neuronal phenotypes. Furthermore, it is also notable that many neuronal signaling proteins (*e.g.* Ras, Rho, paralemmin, and PSD-95) have been modified by the addition of long fatty acid chains including prenylation and palmitoylation (52, 53). These post-translational modifications are suggested to play a critical role for precise membrane localization especially in highly polarized neuronal cells.

What could be the biological significance of such membrane targeting of a CaMK? In the case of Ras, *CAAX* box-dependent membrane anchoring was absolutely required to allow proper membrane recruitment of its downstream kinases, c-Raf and B-Raf (23). Similarly, *CAAX*-mediated localization of CLICK-III to the membranes might represent an advantageous mechanism to help tightly couple upstream signals to local downstream phosphorylation targets. In principle, a direct anchoring of CaMK activity to various membrane compartments is likely to facilitate the synaptic activity-induced local protein phosphorylation at or very close to the site of Ca^{2+} entry/mobilization. Whether such membrane-delimited excitation-phosphorylation coupling can indeed be triggered by electrical activity of the neurons, either postsynaptically or presynaptically, remains to be studied. Alternatively, or additionally, the presence of a CaMK in the Golgi apparatus might enable an efficient coupling of synaptic activity with intracellular trafficking of neuronal proteins. Experiments are underway to provide answers to these issues.

Acknowledgments—We are indebted to Drs. Masaaki Tsuda and Akiko Tabuchi (Toyama Medical and Pharmaceutical University), Dr. Hiroshi Tokumitsu (Kagawa Medical University), and Dr. Ryuichi Shigemoto (National Institute for Physiological Sciences) for comments during the course of the study. We are also grateful to Dr. Hirohide Takebayashi (National Institute for Physiological Sciences) for providing pIRES-S-Tag-EGFP and Dr. Hiroyuki Sakagami (Tohoku University) for sharing unpublished results. We thank Kimiko Nonomura for technical assistance and Tae Arai and Hiroko Nose for secretarial help.

REFERENCES

1. Berridge, M. J., Bootman, M. D., and Lipp, P. (1998) *Nature* **395,** 645–648
2. Bliss, T. V. P., and Collingridge, G. L. (1993) *Nature* **361,** 31–39
3. Schneggenburger, R., Sakaba, T., and Neher, E. (2002) *Trends Neurosci.* **25,** 206–212
4. Bito, H., Deisseroth, K., and Tsien, R. W. (1997) *Curr. Opin. Neurobiol.* **7,** 419–429
5. Bito, H. (1998) *Cell Calcium* **23,** 143–150
6. Soderling, T. R., and Stull, J. T. (2001) *Chem. Rev.* **101,** 2341–2352
7. Hook, S. S, and Means, A. R. (2001) *Annu. Rev. Pharmacol. Toxicol.* **41,** 471–505
8. Kennedy, M. B. (1994) *Annu. Rev. Biochem.* **63,** 571–600
9. Lisman, J., Schulman, H., and Cline, H. (2002) *Nat. Rev. Neurosci.* **3,** 175–190
10. Hudmon, A., and Schulman, H. (2002) *Annu. Rev. Biochem.* **71,** 473–510
11. Malinow, R., and Malenka, R. C. (2002) *Annu. Rev. Neurosci.* **25,** 103–126
12. Silva, A. J., Kogan, J. H., Frankland, P. W., and Kida, S. (1998) *Annu. Rev. Neurosci.* **21,** 127–148
13. Picciotto, M. R., Nastiuk, K. L., and Nairn, A. C. (1996) *Adv. Pharmacol.* **36,** 251–275
14. Fujisawa, H. (2001) *J. Biochem. (Tokyo)* **129,** 193–199
15. Yokokura, H., Terada, O., Naito, Y., Sugita, R., and Hidaka, H. (1997) *Adv. Second Messenger Phosphoprotein Res.* **31,** 151–157
16. Bito, H., Deisseroth, K., and Tsien, R. W. (1996) *Cell* **87,** 1203–1214
17. Picciotto, M. R., Zoli, M., Bertuzzi, G., and Nairn, A. C. (1995) *Synapse* **20,** 75–84
18. Verploegen, S., Lammers, J. W., Koenderman, L., and Coffer, P. J. (2000) *Blood* **96,** 3215–3223
19. Yokokura, H., Terada, O., Naito, Y., and Hidaka H. (1997) *Biochim. Biophys. Acta* **1338,** 8–12
20. Naito, Y., Watanabe, Y., Yokokura, H., Sugita, R., Nishino, M., and Hidaka, H. (1997) *J. Biol. Chem.* **272,** 32704–32708
21. Ueda, T., Sakagami, H., Abe, K., Oishi, I., Maruo, A., Kondo, H., Terashima, T., Ichihashi, M., Yamamura, H., and Minami, Y. (1999) *J. Neurochem.* **73,** 2119–2129
22. Choy, E., Chiu, V. K., Siletti, J., Feoktistov, M., Morimoto, T., Michaelson, D., Ivanov, I. E., and Philips, M. R. (1999) *Cell* **98,** 69–80
23. Zhang, F. L., and Casey, P. J. (1996) *Annu. Rev. Biochem.* **65,** 241–269
24. Tokumitsu, H., Brickey, D. A., Glod, J., Hidaka, H., Sikela, J., and Soderling, T. R. (1994) *J. Biol. Chem.* **269,** 28640–28647
25. Okuno, S., Kitani, T., and Fujisawa, H. (1994) *J. Biochem. (Tokyo)* **116,** 923–930
26. Tokumitsu, H., Enslen, H., and Soderling, T. R. (1995) *J. Biol. Chem.* **270,** 19320–19324
27. Haribabu, B., Hook, S. S., Selbert, M. A., Goldstein, E. G., Tomhave, E. D., Edelman, A. M., Snyderman, R., and Means, A. R. (1995) *EMBO J.* **14,** 3679–3686
28. Edelman, A. M., Mitchelhill, K. I., Selbert, M. A., Anderson, K. A., Hook, S. S., Stapleton, D., Goldstein, E. G., Means, A. R., and Kemp, B. E. (1996) *J. Biol. Chem.* **271,** 10806–10810
29. Matsushita, M., and Nairn, A. C. (1998) *J. Biol. Chem.* **273,** 21473–21481
30. Kitani, T., Okuno, S., and Fujisawa, H. (1997) *J. Biochem. (Tokyo)* **122,** 243–250
31. Anderson, K. A., Means, R. L., Huang, Q. H., Kemp, B. E., Goldstein, E. G., Selbert, M. A., Edelman, A. M., Fremeau, R. T., and Means, A. R. (1998) *J. Biol. Chem.* **273,** 31880–31889
32. Sheng, M., Thompson, M. A., and Greenberg, M. E. (1991) *Science* **252,** 1427–1430
33. Liao, J. K. (2002) *J. Clin. Invest.* **110,** 285–288
34. Oida, H., Namba, T., Sugimoto, Y., Ushikubi, F., Ohishi, H., Ichikawa, A., and Narumiya, S. (1997) *Br. J. Pharmacol.* **116,** 2828–2837
35. Erondu, N. E., and Kennedy, M. B. (1985) *J. Neurosci.* **5,** 3270–3277
36. Nakamura, Y., Okuno, S., Sato, F., and Fujisawa, H. (1995) *Neuroscience* **68,** 181–194
37. Sakagami, H., Umemiya, M., Saito, S., and Kondo, H. (2000) *Eur. J. Neurosci.* **12,** 89–99
38. Harris, K. M. (1999) *Curr. Opin. Neurobiol.* **9,** 343–348
39. Fukunaga, K., Muller, D., and Miyamoto, E. (1995) *J. Biol. Chem.* **270,** 6119–6124
40. Kasahara, J., Fukunaga, K., and Miyamoto, E. (2001) *J. Biol. Chem.* **276,** 24044–24050
41. Deisseroth, K., Bito, H., and Tsien, R. W. (1996) *Neuron* **16,** 89–101
42. Thiagarajan, T. C., Piedras-Renteria, E. S., and Tsien, R. W. (2002) *Neuron* **36,** 1103–1114
43. Ho, N., Liauw, J. A., Blaeser, F., Wei, F., Hanissian, S., Muglia, L. M., Wozniak, D. F., Nardi, A., Arvin, K. L., Holtzman, D. M., Linden, D. J., Zhuo, M., Muglia, L. J., and Chatila, T. A. (2000) *J. Neurosci.* **20,** 6459–6472
44. Ribar, T. J., Rodriguiz, R. M., Khiroug, L., Wetsel, W. C., Augustine, G. J., and Means, A. R. (2002) *J. Neurosci.* **20,** 1–5
45. Kang, H., Sun, L. D., Atkins, C. M., Soderling, T. R., Wilson, M. A., and Tonegawa, S. (2001) *Cell* **106,** 771–783
46. Wei, F., Qiu, C. S., Liauw, J., Robinson, D. A., Ho, N., Chatila, T., and Zhuo, M. (2002) *Nat. Neurosci.* **5,** 573–579
47. Davis, M., and Whalen, P. J. (2001) *Mol. Psychiatry* **6,** 13–34
48. Woods, S. C., and Stricker, E. M. (1999) *Fundamental Neuroscience* (Zigmond, M. J., Bloom, F. E., Landis, S. C., Roberts, J. L., and Squire, L. R., eds) pp. 1090–1101, Academic Press, New York
49. Flanagan-Cato, L. M., Calizo, L. H., and Daniels, D. (2001) *Horm. Behav.* **40,** 178–182
50. Matthies, H. Jr., Schulz, S., Hollt, V., and Krug, M. (1997) *Neuroscience* **79,** 341–346
51. Mauch, D. H., Nagler, K., Schumacher, S., Goritz, C., Muller, E. C., Otto, A., and Pfrieger, F. W. (2001) *Science* **294,** 1354–1357
52. El-Husseini, A. E.-D., and Bredt, D. S. (2002) *Nat. Rev. Neurosci.* **3,** 791–802
53. Kutzleb, C., Sanders, G., Yamamoto, R., Wang, X., Lichte, B., Petrasch-Parwez, E., and Kilimann, M. W. (1998) *J. Cell Biol.* **143,** 795–813

CHURCHILL LIVINGSTONE

Cell Calcium 34 (2003) 425–430

cell calcium

www.elsevier.com/locate/ceca

Ca^{2+}/CREB/CBP-dependent gene regulation: a shared mechanism critical in long-term synaptic plasticity and neuronal survival

Haruhiko Bito [a,b,c,*], Sayaka Takemoto-Kimura [a,c]

[a] *Department of Neurochemistry, University of Tokyo Graduate School of Medicine, Bunkyo-ku, Tokyo 113-0033, Japan*
[b] *PRESTO-Japan Science and Technology Corporation, Bunkyo-ku, Tokyo 113-0033, Japan*
[c] *Department of Pharmacology, Kyoto University Faculty of Medicine, Sakyo-ku, Kyoto 606-8315, Japan*

Received 10 May 2003; accepted 12 May 2003

Abstract

CREB is a transcription factor critical for long-term synaptic plasticity. Intriguingly, recent work has elucidated a role for CREB, as well as upstream CREB kinases, in the control of activity-dependent neuronal survival. Additionally, analysis of the molecular pathology of polyglutamine-repeat diseases suggest that alteration of pCREB–CBP function may underlie, at least in part, the neurodegenerative process. Taken together, these new findings support the idea that Ca^{2+}/CREB/CBP-dependent gene regulation might be a shared mechanism critical in both long-term synaptic plasticity and neuronal survival.

Keywords: Gene regulation; Synaptic plasticity; Neuronal survival; Calcium; CREB; CBP; CaM kinase

1. Introduction

In order to execute a higher cognitive task in response to external and internal stimuli, brain needs to compute an output, based upon a barrage of input information that it receives from the outside world. To be able to successfully compute a correct answer above par on a continuous basis, it has been speculated that there must a mechanism for online storage of data about the input–output relationship of the attended events. Furthermore, it is also believed that "useful" information can be consolidated within a neuronal network, thereby perhaps allowing the brain to store experience as a memory and become smarter. Such stimuli-dependent changes in the brain have been proposed to be acquired by using mechanisms of synaptic plasticity. According to the *synaptic plasticity and memory hypothesis*, "activity-dependent synaptic plasticity is induced at appropriate synapses during memory formation and is both necessary and sufficient for the information storage underlying the type of memory mediated by the brain area in which that plasticity is observed" [1].

In recent years, both activity-induced gene expression/protein synthesis and activity-induced changes in neuronal morphology have received much attention as potential mechanisms likely to play a significant role in synaptic plasticity and long-term memory formation [2]. Experiments in hippocampal pyramidal excitatory neurons have shown that robust electrical activity can induce a large amount of Ca^{2+}-dependent gene expression [3]. A crystal-clear picture of the events following synaptic Ca^{2+} entry still remains missing, as the repertoire of activity-dependent transcription factors is not fully understood. Indeed, the activation mechanisms and the physiological significance have been demonstrated for only a few of them. These include the Ca^{2+}/cAMP-response element-binding protein (CREB) and nuclear factor of activated T-cells (NFAT). In this review, I shall overview some of the key evidence that has recently led to the rather surprising notion that the Ca^{2+}/CREB/CREB-binding protein (CBP) signaling system might constitute a prototypical signaling module critical not only in long-term synaptic plasticity, but also in basic neuronal survival.

2. Physiological significance of CREB-dependent transcription in long-term synaptic plasticity in the CNS

The critical importance of the transcription factor CREB in CNS functions has been suggested from genetic work in different model organisms, such as the mollusk *Aplysia*, the fruitfly *Drosophila melanogaster*, and the mouse. In all these species, disruption of CREB function in neurons was

* Corresponding author. Tel.: +81-3-5841-3559; fax: +81-3-3814-8154.
E-mail address: hbito@m.u-tokyo.ac.jp (H. Bito).

0143-4160/$ – see front matter © 2003 Elsevier Ltd. All rights reserved.
doi:10.1016/S0143-4160(03)00140-4

associated with specific defect in long-term, but not short-term, plasticity or memory [4]. Furthermore, up-regulation of CREB-dependent transcription significantly facilitated the generation of the late phase of long-term potentiation [5].

However, as CREB is not a transcription factor specifically expressed in postmitotic neurons, CREB may also mediate universal functions associated with cell growth and differentiation. Indeed, complete removal of all CREB gene products in a full CREB-knockout (KO) mouse resulted in early embryonic lethality [6]. To circumvent such caveat, a transgenic mouse expressing an inducible form of dominant negative CREB in postmitotic forebrain neurons was recently created. By using this line of mouse, the requirement for CREB was shown not only in consolidation but also in reconsolidation of long-term memory [7]. In addition, the availability of a CRE-lacZ reporter line of transgenic mouse [8] has much facilitated the elucidation of the spatiotemporal activation of CREB-dependent gene expression in many brain areas during long-term memory, as well as visual and barrel cortex plasticity [9–13]. Taken together, CREB-dependent gene expression is likely to play a crucial role in associating synaptic activity with long-term changes in synaptic circuitry in many kinds of neuronal systems.

3. Phosphorylation-dependent control of CREB activity may regulate long-term synaptic plasticity and neuronal survival

How is CREB function regulated by synaptic activity? A clue to this critical question can be obtained by the structure of CREB. Phylogenic analysis of the CREB cDNA from *Caenorhabditis elegans* to mammals revealed a high degree of conservation in at least two domains. In addition to the bZIP leucine zipper domain, a well-conserved stretch of amino acid sequence can be found around the Ser-133 in a domain called kinase-inducible domain (KID) (Fig. 1). Protein kinase A-dependent phosphorylation of this Ser-133 residue was shown to significantly augment the binding affinity of KID with the KID-interacting domain (KIX) in the CBP, a histone acetyltransferase which is associated with the transcriptional preinitiation complex [14,15]. Formation of a stable complex between CREB and CBP by increasing the affinity of the physical interface between the two proteins has been demonstrated to lie at heart of CREB-dependent gene expression [16–18]. CREB–CBP interaction may be further modified by additional covalent modifications of CREB such as phosphorylation of Ser-142/Ser-143 [19,20], protein phosphatase 1-dependent dephosphorylation of Ser-133 [21,22], or acetylation of lysine residues [23].

Downstream of synaptic Ca^{2+} entry, a CaMKK/CaMKIV plays a critical role in activity-dependent phosphorylation of CREB [22]. Recent reports using either a transgenic mouse carrying a dominant negative CaMKIV allele downstream of a CaMKII promoter [24], or two separate lines of CaMKIV-KO mice [25,26], now provide clear independent support for the model that CaMKIV-dependent CREB activation is necessary for long-term synaptic plasticity in the hippocampus [24,25] and young Purkinje neurons [25], and long-term spatial and fear memory [24,27]. The identity of the responsible CaMK involved in CREB phosphorylation may be extended, under certain circumstances, to other CaMK of the CaMKI/IV family such as CaMKIα, CaMKIβ2, or CLICK-III/CaMKIγ, as these have been shown to couple with CREB-dependent gene expression, at least in a heterologous system or in *C. elegans* [28–32].

Better understanding of the mode of activation of CREB has led to creation of potent dominant negative constructs of CREB [33]. Overexpression of these dominant negative alleles have shown an unexpected role of CREB in prevention from apoptosis in cultured neurons [34,35]. Consistent with these reports, a full CREB-KO mice showed a significant increase in neuronal cell death in dorsal root ganglion neurons [36]. Furthermore, a floxed CREB-knock in mouse in was produced in a CREM-null background in the Schutz laboratory. When this line was crossed with neuronal Cre-driver lines, ablation of neuronal CREB during development resulted in a massive neuronal apoptosis, whereas Cre expression in postmitotic neurons led to a progressive neurodegeneration [37]. Taken together, these lines of evidence collectively suggest a requirement of CREB-dependent gene expression in the maintenance of neuronal cell population during CNS development, as well as following synaptogenesis and neuronal wiring.

Does the involvement of CREB in neuronal survival require neuronal activity and synaptic calcium influx? The reports mentioned above did not directly address this question. Rather, the evidence implicated neurotrophins such as nerve growth factor (NGF) and brain-derived growth factor (BDNF), or growth factors such as insulin-like growth factor-1 as signal ligands upstream of CREB, and thus a Ras-MAPK-RSK2 signaling cascade seemed to be sufficient to convey the necessary pCREB signal flow for survival (Fig. 2).

4. CaMKIV-mediated CREB phosphorylation contributes to survival of cerebellar granule cells in vitro

In collaboration with the Loeffler laboratory, we recently tested the involvement of activity-induced CREB activation mechanisms in neuronal survival, under experimental conditions where depolarization with high K^+ concentration and a subsequent Ca^{2+} influx helped maintain the survival of cerebellar granule cells. In this model system, treatment with Ca^{2+} channel antagonists of the dihydropyridine class, such as nimodipine or nifedipine, but not with ω-conotoxin MVIIC, showed effects similar to K^+ deprivation. Thus, it was proposed that Ca^{2+} entry via L-type, but not via N/P/Q-type, Ca^{2+} channels may be essential to trigger activation of a specific signaling cascade leading to neuronal survival. As predicted from this model, either elevation of

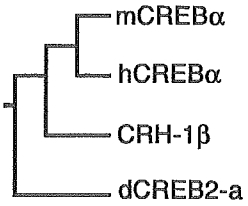

KID domain

```
                                        *
mCREBα      113  ESVDSVTDSQKRREILSRRPSYRKILNDLSSDAPGVPRIEEE  154
hCREBα      113  ESVDSVTDSQKRREILSRRPSYRKILNDLSSDAPGVPRIEEE  154
CRH-1β        9  EGGDSEDEARRRREQLNRRPSYRMILKDLETADKVMKKEPEE   50
apCREB1α     65  DLSSSDSDAKKRREILTRRPSYRKILNELSSPVSKMDDDSNS  106
dCREB2-a    211  DESLSDDDSQHHRSELTRRPSYNKIFTELSGPDMSGASLPMS  252
```

bZIP domain

```
                                                  *       *
mCREBα      280  EEAARKREVRLMKNREAARECRRKKKEYVKCLENRVAVLENQ  321
hCREBα      280  EEAARKREVRLMKNREAARECRRKKKEYVKCLENRVAVLENQ  321
CRH-1β      242  DESNRKRQVRLLKNREAAKECRRKKKEYVKCLENRVSVLENQ  283
apCREB1α    210  EEGSRKRELRLLKNREAARECRRKKKEYVKCLENRVAVLENQ  251
dCREB2-a    298  EDQTRKREIRLQKNREAARECRRKKKEYIKCLENRVAVLENQ  339

                    *       *
mCREBα      322  NKTLIEELKALKDLYCHKSD      341
hCREBα      322  NKTLIEELKALKDLYCHKSD      341
CRH-1β      284  NKALIEELKTLKELYCRKEKDGM   306
apCREB1α    252  NKTLIEELKALKELYCQKDA      271
dCREB2-a    340  NKALIEELKSLKELYCQTKND     360
```

Fig. 1. Conservation of CREB protein during evolution. The top panel shows a phylogenic analysis of full-length CREB amino acid sequences using Clustal W. It is likely that *D. melanogaster* CREB ortholog (dCREB2-a) has evolved separately from the mammalian CREB (mCREBα, hCREBα) gene, as the *C. elegans* full-length CREB protein (CRH-1β) has higher homology with its mammalian, rather than the fruitfly, counterpart. The KID and the bZIP domains show overall a remarkable degree of conservation, as shown in the lower panels. Marked in red and green are identical and conserved amino acid residues, respectively. Ser-133 and the leucine residues forming a leucine zipper are shown with an asterisk.

extracellular K^+ concentration or facilitation of L-type Ca^{2+} current with FPL64176 indeed significantly augmented survival of cerebellar granule neurons, in inverse correlation with caspase activity [38].

As calmodulin (CaM) had been proposed to be required for calcium-dependent cell survival [39], we examined the potential role of several Ca^{2+}/calmodulin-dependent protein kinases (CaMKs) in mediating the Ca^{2+}/CaM effects. We were particularly interested in CaMKIV as CaMKIV has been shown to be predominantly expressed in the cerebellar granule cells, and furthermore, CaMKIV was demonstrated in various cell systems to trigger phosphorylation of CREB downstream of synaptic Ca^{2+}-influx or massive depolarization using high K^+ [22,40,41]. Contribution of Ras/MAPK/Rsk2 was also suggested for a late phase of activity-dependent CREB phosphorylation [41].

Intriguingly, induction of apoptosis by K^+ deprivation in cerebellar granule neurons resulted in a time-dependent degradation and proteolysis of CaMKIV, in a caspase 3-dependent manner [38]. As a result, basal pCREB amount was reduced significantly. Conversely, either opening of L-type Ca^{2+} channels or treatment of caspase-3 inhibitors prevented CaMKIV degradation as well as decrease in basal pCREB. As dominant active forms of either CaMKIV or CREB rescued K^+-deprivation-induced apoptosis, while dominant negative forms of CaMKIV or CREB induced apoptosis even under high K^+ conditions, it was suggested that a Ca^{2+}/CaMKIV/CREB pathway contributed in tightly controlling the amount of basal CREB-dependent

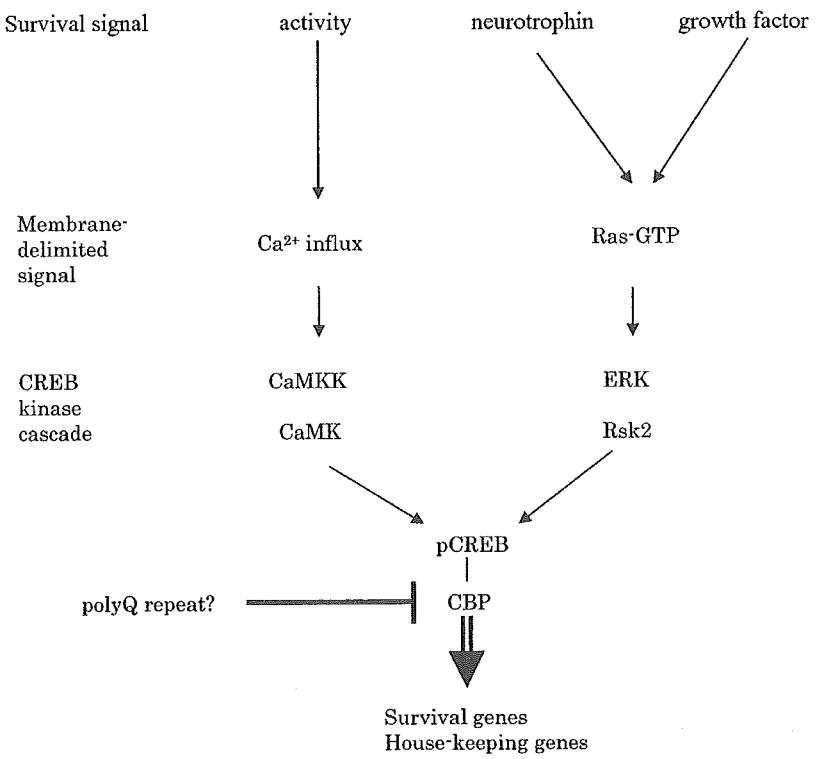

Fig. 2. Convergence of survival signals onto the CREB/CBP-signaling module. Various kinds of neuronal survival factors such as activity, neurotrophins or growth factors induce specific membrane-delimited signals that triggers and converge onto CREB phosphorylation. Phosphorylated CREB, by virtue of an increased affinity to CBP, a co-activator, can then turn of transcription of a battery of survival as well as house-keeping genes. In polyQ-diseases, the efficiency of pCREB–CBP interaction may be diminished, thus creating a deficit in the pool of CREB-dependent survival genes. This may create an increased susceptibility to insults, thereby augmenting the chance for neuronal death in the long run.

gene expression that was required for neuronal survival. The participation of MAPK/Rsk2 pathway in this form of activity-induced neuronal survival still remains to be shown.

5. Are neurodegeneration in polyglutamine diseases CREBopathies?

Neuronal apoptosis, characterized by nuclear condensation and fragmentation, is a common hallmark of neurons affected with neurodegenerative diseases, such as Alzheimer's or Huntington's disease. In recent years, understanding of the molecular pathology of polyglutamine repeat-diseases has made a tremendous progress. One recent achievement was the realization that polyglutamine repeat-containing proteins strongly interfered with many component of the basal transcriptional complex. PolyQ stretches were found to be able to strongly bind $TAF_{II}130$, a coactivator of the basal transcriptional machinery known to interact with CREB, thereby significantly interfering with CREB-dependent transcriptional activation [42]. On the other hand, huntingtin, a gene product whose mutation is known to cause Huntington's disease, was shown to interact with CBP, and to cause mislocalization and repression of CBP-mediated transcription [43–45]. Thus, gradual attenuation of CREB/CBP-mediated gene expression by misrecruitment of CREB-binding general transcription factors and coactivators into the polyQ-enriched aggregates now appears to be one of major pathological features of the triplet-repeat overexpressing cells [46] (Fig. 2). Consistent with a causative role for CREB/CBP-dysfunction in triplet-triggered diseases, complete removal of CREB in postnatal mouse brain by a Cre-Lox strategy in a CREM-null background generated a slow progressive degeneration in the striatum reminiscent of Huntington's disease phenotype [37]. Conversely, pharmacological intervention to restore the diminished histone acetylase activity of CBP seems to successfully stop the neurondegenerative process in model cells and animals [47,48]. As degradation of CaMKIV [38], CREB [49] or CBP [50] is found to correlate with neuronal death, restoration and maintenance of the Ca^{2+}/CREB/CBP system may thus constitute a bona fide physiological strategy to enhance survival of neurons, and prevent their pathological death.

Acknowledgements

We are grateful to Violaine Sée, Anne-Laurence Boutillier and Jean-Philippe Loeffler, with whom we originally initiated our study on calcium-dependent control of cell survival, and Shoji Tsuji for discussion. We thank Shuh Narumiya for support, members of the Neuroscience Unit at the Department of Pharmacology Kyoto University

Faculty of Medicine for continuous encouragements, Kimiko Nonomura for technical assistance, and Tae Arai and Hiroko Nose for secretarial assistance. We apologize to numerous authors whose papers we could not cite due to space limitations. This work was supported by Grants-in-Aid from the Ministry of Education, Culture, Sports, Science and Technology and the Ministry of Health, Labour and Welfare of Japan, a PRESTO investigatorship from the Japan Science and Technology Corporation, and a Human Frontier Science Program grant. S.T.-K. is a predoctoral fellow from the Japan Society for Promotion of Science.

References

[1] S.J. Martin, P.D. Grimwood, R.G. Morris, Synaptic plasticity and memory: an evaluation of the hypothesis, Annu. Rev. Neurosci. 23 (2000) 649–711.
[2] E.R. Kandel, The molecular biology of memory storage: a dialogue between genes and synapses, Science 294 (2001) 1030–1038.
[3] H. Bito, The role of calcium in activity-dependent neuronal gene regulation, Cell Calcium 23 (1998) 143–150.
[4] A.J. Silva, J.H. Kogan, P.W. Frankland, S. Kida, CREB and memory, Annu. Rev. Neurosci. 21 (1998) 127–148.
[5] A. Barco, J.M. Alarcon, E.R. Kandel, Expression of constitutively active CREB protein facilitates the late phase of long-term potentiation by enhancing synaptic capture, Cell 108 (2002) 689–703.
[6] D. Rudolph, A. Tafuri, P. Gass, G.J. Hammerling, B. Arnold, G. Schutz, Impaired fetal T cell development and perinatal lethality in mice lacking the cAMP response element binding protein, Proc. Natl. Acad. Sci. U.S.A. 95 (1998) 4481–4486.
[7] S. Kida, S.A. Josselyn, S.P. de Ortiz, J.H. Kogan, I. Chevere, S. Masushige, A.J. Silva, CREB required for the stability of new and reactivated fear memories, Nat. Neurosci. 5 (2002) 348–355.
[8] S. Impey, M. Mark, E.C. Villacres, S. Poser, C. Chavkin, D.R. Storm, Induction of CRE-mediated gene expression by stimuli that generate long-lasting LTP in area CA1 of the hippocampus, Neuron 16 (1996) 973–982.
[9] S. Impey, D.M. Smith, K. Obrietan, R. Donahue, C. Wade, D.R. Storm, Stimulation of cAMP response element (CRE)-mediated transcription during contextual learning, Nat. Neurosci. 1 (1998) 595–601.
[10] T.A. Pham, S. Impey, D.R. Storm, M.P. Stryker, CRE-mediated gene transcription in neocortical neuronal plasticity during the developmental critical period, Neuron 22 (1999) 63–72.
[11] A.L. Barth, M. McKenna, S. Glazewski, P. Hill, S. Impey, D. Storm, K. Fox, Upregulation of cAMP response element-mediated gene expression during experience-dependent plasticity in adult neocortex, J. Neurosci. 20 (2000) 4206–4216.
[12] J. Athos, S. Impey, V.V. Pineda, X. Chen, D.R. Storm, Hippocampal CRE-mediated gene expression is required for contextual memory formation, Nat. Neurosci. 5 (2002) 1119–1120.
[13] R. Lamprecht, S. Hazvi, Y. Dudai, cAMP response element-binding protein in the amygdala is required for long- but not short-term conditioned taste aversion memory, J. Neurosci. 17 (1997) 8443–8450.
[14] B. Mayr, M. Montminy, Transcriptional regulation by the phosphorylation-dependent factor CREB, Nat. Rev. Mol. Cell. Biol. 2 (2001) 599–609.
[15] A.J. Shaywitz, M.E. Greenberg, CREB: a stimulus-induced transcription factor activated by a diverse array of extracellular signals, Annu. Rev. Biochem. 68 (1999) 821–861.
[16] J.R. Cardinaux, J.C. Notis, Q. Zhang, N. Vo, J.C. Craig, D.M. Fass, R.G. Brennan, R.H. Goodman, Recruitment of CREB binding protein is sufficient for CREB-mediated gene activation, Mol. Cell Biol. 20 (2000) 1546–1552.
[17] K. Du, H. Asahara, U.S. Jhala, B.L. Wagner, M. Montminy, Characterization of a CREB gain-of-function mutant with constitutive transcriptional activity in vivo, Mol. Cell Biol. 20 (2000) 4320–4327.
[18] A.J. Shaywitz, S.L. Dove, J.M. Kornhauser, A. Hochschild, M.E. Greenberg, Magnitude of the CREB-dependent transcriptional response is determined by the strength of the interaction between the kinase-inducible domain of CREB and the KIX domain of CREB-binding protein, Mol. Cell Biol. 20 (2000) 9409–9422.
[19] J.M. Kornhauser, C.W. Cowan, A.J. Shaywitz, R.E. Dolmetsch, E.C. Griffith, L.S. Hu, C. Haddad, Z. Xia, M.E. Greenberg, CREB transcriptional activity in neurons is regulated by multiple calcium-specific phosphorylation events, Neuron 34 (2002) 221–233.
[20] D. Gau, T. Lemberger, C. von Gall, O. Kretz, N. Le Minh, P. Gass, W. Schmid, U. Schibler, H.W. Korf, G. Schutz, Phosphorylation of CREB Ser142 regulates light-induced phase shifts of the circadian clock, Neuron 34 (2002) 245–253.
[21] M. Hagiwara, A. Alberts, P. Brindle, J. Meinkoth, J. Feramisco, T. Deng, M. Karin, S. Shenolikar, M. Montminy, Transcriptional attenuation following cAMP induction requires PP-1-mediated dephosphorylation of CREB, Cell 70 (1992) 105–113.
[22] H. Bito, K. Deisseroth, R.W. Tsien, CREB phosphorylation and dephosphorylation: a Ca^{2+}- and stimulus duration-dependent switch for hippocampal gene expression, Cell 87 (1996) 1203–1214.
[23] Q. Lu, A.E. Hutchins, C.M. Doyle, J.R. Lundblad, R.P. Kwok, Acetylation of CREB by CBP enhances CREB-dependent transcription, J. Biol. Chem. 2003, in press.
[24] H. Kang, L.D. Sun, C.M. Atkins, T.R. Soderling, M.A. Wilson, S. Tonegawa, An important role of neural activity-dependent CaMKIV signaling in the consolidation of long-term memory, Cell 106 (2001) 771–783.
[25] N. Ho, J.A. Liauw, F. Blaeser, F. Wei, S. Hanissian, L.M. Muglia, D.F. Wozniak, A. Nardi, K.L. Arvin, D.M. Holtzman, D.J. Linden, M. Zhuo, L.J. Muglia, T.A. Chatila, Impaired synaptic plasticity and cAMP response element-binding protein activation in Ca^{2+}/calmodulin-dependent protein kinase type IV/Gr-deficient mice, J. Neurosci. 20 (2000) 6459–6472.
[26] T.J. Ribar, R.M. Rodriguiz, L. Khiroug, W.C. Wetsel, G.J. Augustine, A.R. Means, Cerebellar defects in Ca^{2+}/calmodulin kinase IV-deficient mice, J. Neurosci. 20 (2000) RC107.
[27] F. Wei, C.S. Qiu, J. Liauw, D.A. Robinson, N. Ho, T. Chatila, M. Zhuo, Calcium calmodulin-dependent protein kinase IV is required for fear memory, Nat. Neurosci. 5 (2002) 573–579.
[28] B. Haribabu, S.S. Hook, M.A. Selbert, E.G. Goldstein, E.D. Tomhave, A.M. Edelman, R. Snyderman, A.R. Means, Human calcium-calmodulin dependent protein kinase I: cDNA cloning, domain structure and activation by phosphorylation at threonine-177 by calcium-calmodulin dependent protein kinase I kinase, EMBO J. 14 (1995) 3679–3686.
[29] M. Matsushita, A.C. Nairn, Characterization of the mechanism of regulation of Ca^{2+}/calmodulin-dependent protein kinase I by calmodulin and by Ca^{2+}/calmodulin-dependent protein kinase kinase, J. Biol. Chem. 273 (1998) 21473–21481.
[30] Y. Naito, Y. Watanabe, H. Yokokura, R. Sugita, M. Nishio, H. Hidaka, Isoform-specific activation and structural diversity of calmodulin kinase I, J. Biol. Chem. 272 (1997) 32704–32708.
[31] S. Takemoto-Kimura, H. Terai, M. Takamoto, S. Ohmae, S. Kikumura, E. Segi, Y. Arakawa, T. Furuyashiki, S. Narumiya, H. Bito, Molecular cloning and characterization of CLICK-III/CaMKIγ, a novel membrane-anchored neuronal CaMK, J. Biol. Chem. 278 (2003) 18597–18605.
[32] Y. Kimura, E.E. Corcoran, K. Eto, K. Gengyo-Ando, M.A. Muramatsu, R. Kobayashi, J.H. Freedman, S. Mitani, M. Hagiwara, A.R. Means, H. Tokumitsu, A CaMK cascade activates CRE-mediated transcription in neurons of *Caenorhabditis elegans*, EMBO Rep. 3 (2002) 962–966.

[33] S. Ahn, M. Olive, S. Aggarwal, D. Krylov, D.D. Ginty, C. Vinson, A dominant-negative inhibitor of CREB reveals that it is a general mediator of stimulus-dependent transcription of c-fos, Mol. Cell Biol. 18 (1998) 967–977.

[34] A. Bonni, A. Brunet, A.E. West, S.R. Datta, M.A. Takasu, M.E. Greenberg, Cell survival promoted by the Ras-MAPK signaling pathway by transcription-dependent and -independent mechanisms, Science 286 (1999) 1358–1362.

[35] A. Riccio, S. Ahn, C.M. Davenport, J.A. Blendy, D.D. Ginty, Mediation by a CREB family transcription factor of NGF-dependent survival of sympathetic neurons, Science 286 (1999) 2358–2361.

[36] B.E. Lonze, A. Riccio, S. Cohen, D.D. Ginty, Apoptosis, axonal growth defects, and degeneration of peripheral neurons in mice lacking CREB, Neuron 34 (2002) 371–385.

[37] T. Mantamadiotis, T. Lemberger, S.C. Bleckmann, H. Kern, O. Kretz, A. Martin Villalba, F. Tronche, C. Kellendonk, D. Gau, J. Kapfhammer, C. Otto, W. Schmid, G. Schutz, Disruption of CREB function in brain leads to neurodegeneration, Nat. Genet. 31 (2002) 47–54.

[38] V. Sée, A.L. Boutillier, H. Bito, J.P. Loeffler, Calcium/calmodulin-dependent protein kinase type IV (CaMKIV) inhibits apoptosis induced by potassium deprivation in cerebellar granule neurons, FASEB J. 15 (2001) 134–144.

[39] A.L. Boutillier, P. Kienlen-Campard, J.P. Loeffler, Depolarization regulates cyclin D1 degradation and neuronal apoptosis: a hypothesis about the role of the ubiquitin/proteasome signalling pathway, Eur. J. Neurosci. 11 (1999) 441–448.

[40] K. Deisseroth, E.K. Heist, R.W. Tsien, Translocation of calmodulin to the nucleus supports CREB phosphorylation in hippocampal neurons, Nature 392 (1998) 198–202.

[41] G.Y. Wu, K. Deisseroth, R.W. Tsien, Activity-dependent CREB phosphorylation: convergence of a fast, sensitive calmodulin kinase pathway and a slow, less sensitive mitogen-activated protein kinase pathway, Proc. Natl. Acad. Sci. U.S.A. 98 (2001) 2808–2813.

[42] T. Shimohata, T. Nakajima, M. Yamada, C. Uchida, O. Onodera, S. Naruse, T. Kimura, R. Koide, K. Nozaki, Y. Sano, H. Ishiguro, K. Sakoe, T. Ooshima, A. Sato, T. Ikeuchi, M. Oyake, T. Sato, Y. Aoyagi, I. Hozumi, T. Nagatsu, Y. Takiyama, M. Nishizawa, J. Goto, I. Kanazawa, I. Davidson, N. Tanese, H. Takahashi, S. Tsuji, Expanded polyglutamine stretches interact with TAFII130, interfering with CREB-dependent transcription, Nat. Genet. 26 (2000) 29–36.

[43] A. McCampbell, J.P. Taylor, A.A. Taye, J. Robitschek, M. Li, J. Walcott, D. Merry, Y. Chai, H. Paulson, G. Sobue, K.H. Fischbeck, CREB-binding protein sequestration by expanded polyglutamine, Hum. Mol. Genet. 9 (2000) 2197–2202.

[44] J.S. Steffan, A. Kazantsev, O. Spasic-Boskovic, M. Greenwald, Y.Z. Zhu, H. Gohler, E.E. Wanker, G.P. Bates, D.E. Housman, L.M. Thompson, The Huntington's disease protein interacts with p53 and CREB-binding protein and represses transcription, Proc. Natl. Acad. Sci. U.S.A. 97 (2000) 6763–6768.

[45] F.C. Nucifora Jr., M. Sasaki, M.F. Peters, H. Huang, J.K. Cooper, M. Yamada, H. Takahashi, S. Tsuji, J. Troncoso, V.L. Dawson, T.M. Dawson, C.A. Ross, Interference by huntingtin and atrophin-1 with CBP-mediated transcription leading to cellular toxicity, Science 291 (2001) 2423–2428.

[46] T. Shimohata, O. Onodera, S. Tsuji, Expanded polyglutamine stretches lead to aberrant transcriptional regulation in polyglutamine diseases, Hum. Cell 14 (2001) 17–25.

[47] J.S. Steffan, L. Bodai, J. Pallos, M. Poelman, A. McCampbell, B.L. Apostol, A. Kazantsev, E. Schmidt, Y.Z. Zhu, M. Greenwald, R. Kurokawa, D.E. Housman, G.R. Jackson, J.L. Marsh, L.M. Thompson, Histone deacetylase inhibitors arrest polyglutamine-dependent neurodegeneration in *Drosophila*, Nature 413 (2001) 739–743.

[48] A. McCampbell, A.A. Taye, L. Whitty, E. Penney, J.S. Steffan, K.H. Fischbeck, Histone deacetylase inhibitors reduce polyglutamine toxicity, Proc. Natl. Acad. Sci. U.S.A. 98 (2001) 15179–15184.

[49] V. Sée, J.P. Loeffler, Oxidative stress induces neuronal death by recruiting a protease and phosphatase-gated mechanism, J. Biol. Chem. 276 (2001) 35049–35059.

[50] H. Jiang, F.C. Nucifora, C.A. Ross, D.B. DeFranco, Cell death triggered by polyglutamine-expanded huntingtin in a neuronal cell line is associated with degradation of CREB-binding protein, Hum. Mol. Genet. 12 (2003) 1–12.

JB Minireview—Signal Transduction Underlying Cell Morphogenesis *J. Biochem.* 134, 315–319 (2003)
DOI: 10.1093/jb/mvg147

Dynamic Control of Neuronal Morphogenesis by Rho Signaling

Haruhiko Bito*
Department of Neurochemistry, the University of Tokyo Graduate School of Medicine, 7-3-1 Hongo, Bunkyo-ku, Tokyo 113-0033; and PRESTO-Japan Science and Technology Corporation

Received August 8, 2003; accepted August 15, 2003

Polarization of the neuronal cell body and initiation of the first neuritic process represent the starting point of a series of dynamic metamorphic events by which the newly acquired identity of a group of neurons can be translated into a morphologically complex web of three-dimensional neuronal circuit. Despite the critical importance of these events, little is known about the molecular signaling mechanisms that either regulate the temporal sequence of these steps or ensure the accuracy and the spatial consistency of the resulting circuits. In this review, based on recent findings from our group and others, we present a working model on how the initial events in neuronal morphogenesis in the CNS may be controlled by multiple Rho pathways.

Key words: actin, axon outgrowth, cerebellar granule neurons, mDia1, ROCK.

Almost a century ago, Ramon y Cahal realized the immense potential that the mammalian central nervous system (CNS) acquired during development by virtue of connecting many neuronal cell types with extremely diverse morphology. Since then, a flurry of knowledge has been obtained, both at the physiological and biochemical levels, about the nature of the brain and neurons. Recent progress in cellular genetics makes it even possible to now envisage therapeutic usefulness for re-engineered neural stem cells in the fight against many debilitating diseases of the CNS.

During its lifetime, a neuron has to undergo numerous steps through which it ultimately distinguishes itself from all the other cells of the body (*1*). The first critical series of steps concerns the end of self-renewal whilst being a neuronal progenitor, then its exit from cell cycle, closely followed by its final cell fate choice. Recent advances have established that a complex network of transcription factors and trophic determinants controls the temporal sequence and the spatial spreading of these events. Taking advantage of these findings, several groups have now reported the successful propagation and derivatization *en masse* of various types of neurons out from embryonic as well as neural stem cells.

Astonishing, however, still remains our lack of insights concerning the molecular mechanisms controlling a second critical series of steps in neuronal development, namely the nascence of the first neuritic processes in a central neuron (*2*, *3*). Indeed, few studies have focused on the molecular events critical for understanding how and when an axon is formed. In contrast, once an axon is born, work from a number of laboratories have identified an essential role for molecular gradients formed by instuctive cues such as netrins, slits, semaphorins, ephrins, neurotrophins and chemokines during the guidance of this axon (*e.g. 4–8*).

*For correspondence: Tel: +81-3-5841-3559, Fax: +81-3-3814-8154, E-mail: hbito@m.u-tokyo.ac.jp

Essential role for Rho-family GTPases in neuronal morphogenesis

How does a neuron shape itself? A dynamic morphological alteration is initiated during the acquisition of neuronal polarity and must continue till the completion of synaptogenesis. Rearrangement of actin and microtubule cytoskeleton clearly lies at the heart of such neuronal morphogenesis (*9*, *10*). This is also a critical moment in neuronal network generation since process generation and cell body migration must be spatially and temporally orchestrated in order to achieve patterned formation of neuronal cell layers and appropriate wiring through synapses (*1*, *4–6*).

Recent findings from work in cultured cells and in intact organisms indicate an important role for the antagonism between Rac and Rho GTPases during these steps (*11–16*) (Fig. 1). However, to date, a clear understanding regarding what specific effectors of the small GTPases contribute to each of these opposing signaling events is still missing. Furthermore, whether Rho always antagonizes with Rac remains controversial (see *e.g. 17*, *18*). In keeping with the critical role for the small GTPases, in humans, several hereditary forms of mental retardation or cognitive dysfunction have been linked to molecular components of the Rho signaling such as the RhoGAP oligophrenin-1 (*19*), the RhoGEF ARHGEF6 (*20*), or downstream effectors in the small G protein pathways PAK3 (*21*), LIMK-1 (*22*, *23*), or FMR1 (*24*). However, a clear molecular picture as to the exact role of each different small GTPase pathway is not yet established. As a matter of fact, most small GTPases are abundantly expressed early during development, especially in the brain and are known to have an extensive cross-talk between each other, thus rendering it challenging to crack the fine details of their combinatorial code and hierarchal cascade during any morphogenetic processes.

Control of earliest neuritogenesis by the Rho/ROCK pathway

In recent years, a number of studies have examined the morphological phenotypes associated with overexpression of Rho and related small GTPases in various

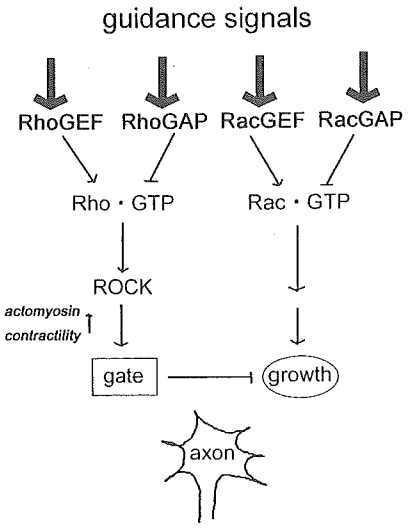

Fig. 1. **Classical view for the role of Rho family GTPases in axon growth.** Recent evidence shows that most guidance molecules are able to modulate small G proteins by acting either on a GEF or a GAP protein. ROCK, a Rho-associated kinase, invariably lies downstream of Rho and gates the ability of Rac-dependent signals to promote axonogenesis and axon growth.

types of neuronal cells, *in vitro* and *in vivo*. Resulting perturbations in neuronal morphogenesis as well as differential effects on actin, myosin, microtubules, or membrane trafficking were then usually attributed to the specific overexpressed small GTPase type. In central neurons, it has now become clear that up- and downregulation of the Rho or ROCK, one of its downstream effectors, dramatically alters axon outgrowth (*25*). In cerebellar granule neurons, strong activation of Rho or ROCK, by overexpression of their dominant active mutants or applying a high dose of an endogenous Rho activator such as SDF-1α, opposes and delays axonogenesis (*25*, *26*). Conversely, downregulation of Rho or ROCK immediately promotes initiation of neuritogenesis and promotes axon outgrowth (*25*, *27*, *28*), presumably by reducing the stability of the cortical actin network in the round neuron (Fig. 1).

Interestingly, the number of axons in cerebellar granule neurons is physiologically set at *two*, a figure that is just in between the number of axons reached with maximal Rho activity (*zero* axon) or minimal Rho activity (*four* or *five* axons). This is in keeping with the finding that constitutive Rho activity level remains relatively high in neurons throughout neuritogenesis (*29*). The elevated level of basal Rho and ROCK activity promotes a high degree of tonic actomyosin contractility (*30*, *31*), thereby setting an efficient gate that may help constrain the timing and the number of axonal outputs coming out from the cell body (Fig. 1), especially in neurons positioned most closely to the pia mater that contains the highest amount of the chemokine SDF-1α. Distancing away from the source of the chemokine gradient during the postnatal expansion of the cerebellar layers may *per se* play a significant part in triggering axonogenesis *in vivo* selectively at the utmost inner layer of the external granule cell layer (Fig. 2, upper panel).

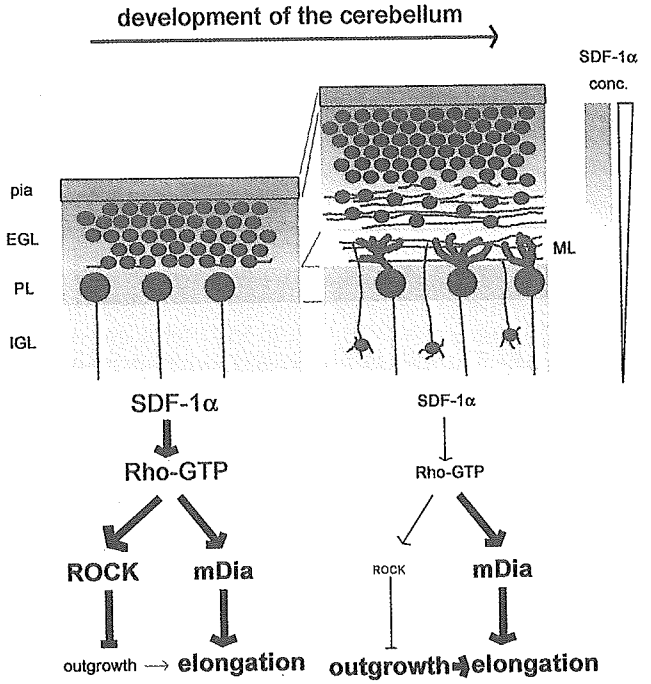

Fig. 2. **A schematic diagram illustrating how the balance between two opposing Rho effectors, ROCK and mDia1, could, in principle, help coordinate formation and elongation of bipolar axons at the utmost inner layer of the external granule cell layer (EGL) in the cerebellum.** Early in the development of the cerebellum when the EGL is still thin, SDF-1α which is heavily expressed in the pia mater (pia), provides a potent Rho-activating signal that prevents axonogenesis via strong activation of ROCK. However, as the EGL expands in size, the SDF-1α concentration near the Purkinje cell layer (PL) becomes more and more reduced, thereby allowing activity of Rho and ROCK to fall within a range where initiation of the first and second axons can occur. However, the residual Rho activity is likely to be sufficient to maintain a high level of mDia1 activity. Such condition would be ideally suited to promote coordinated outgrowth and elongation of parallel fibers, while still keeping the number of axons up to two.

Coordination of axon elongation via ROCK and mDia1

The significance of Rho pathway may not be restricted to negative regulation of axonogenesis. Additionally, ROCK critically controls the motility of axonal growth cones at the tip of extending axons (*25*, *32*). This process was suggested to be mechanistically somewhat distinct from the elongation of the newly formed axons, at least in the context of cerebellar granule neurons, as the latter was significantly facilitated (rather than repressed) in the presence of SDF-1α, a physiological Rho activator in the culture medium (*26*). Curiously, this facilitation correlated with an increase in Rho, rather than Rac activity, and was blocked by the Rho-inhibiting exoenzyme C3. Thus, the existence a Rho-dependent axon elongation mechanism was unexpectedly suggested in central neurons. And the Rho effector critical for mediating this effect was shown to be mDia1, an adaptor protein (*33*, *34*) enriched in cerebellar granule neurons (*26*, *35*).

This raises a rather interesting cell biological question: how can Rho in fact mediate *both* stimulation *and* inhibition of axon outgrowth, via two functionally antagonizing

effectors mDia1 and ROCK (*26*, *36*, *37*)? One factor to consider is the presumed distinct localization of these two Rho effectors within a neuron, as ROCK seems to be expressed diffusely in a cell, while mDia1 was concentrated in the growth cones (*26*). Additionally, the two effectors may differ in their responsiveness to intracellular Rho activity: indeed, it was shown that mDia-based axon elongation was induced by a SDF-1α concentration lower than that required for eliciting ROCK-based inhibition of axon outgrowth, at least in cerebellar granule neurons (*26*). As mDia-Rho binding domain (RBD) bound Rho-GTP tighter than did ROCK-RBD (*38*), one might speculate that the biphasic phenotype could, in principle, result from distinct Rho-GTP affinity of the two effectors (Fig. 2, lower panel).

Rho/mDia1-dependent remodeling of actin structures and microtubules may be crucial in the assembly of cytoskeletal scaffold required for axon outgrowth

How does mDia1, an adaptor protein, exert its effect on axon elongation? mDia1 is a prototypical member of a class of adaptor proteins called formins that contain multiple formin homology domains FH1, FH2 and FH3 (*33*, *34*, *39*). Mutations in various formin proteins in yeasts, flies and worms result in aberrant cell polarity and cytoskeletal remodeling during heavy metamorphic events such as cytokinesis or budding (*40–46*), suggesting that formins exert their effects via control of the actin and microtubule network. Indeed, in Saccharomyces cerevisiae, the Diaphanous homolog Bni1p was shown to be critically involved in controlling actin assembly and the formation of actin cables required for establishment of cell polarity and directed growth (*45*, *47*, *48*). Most remarkable, however, is the recent revelation that the FH2 domain of mDia and other ortholog proteins acts as potent and direct actin nucleators *in vitro*, in an Arp2/3-independent manner. FH2 domain seems to facilitate growth of nucleated actin filaments from the barbed ends, where it remains physically bound without blocking actin polymerization (*49–53*). As a result, continued elongation of unbranched microfilaments is obtained. The actin structure that formins organize seems to be distinct among species: Bni1p assembles actin cables in budding yeast, while mDia1 facilitates formation of stress fibers in mammalian fibroblasts.

Notwithstanding these differences, mDia1, like Bni1p in the bud of the yeast, localizes to the growing end of the cellular cortex in the round neuron and also to the growth cones. Thus it is likely that mDia1 helps tether the actin filaments it nucleates in a polarized manner, through its binding to the barbed ends of the nucleated filaments (*54*). Such mDia1-based polarization of assembled actin microfilaments may play a crucial role in the organization of an early cytoskeletal scaffold required for axon outgrowth.

In yeast, the polarized actin structures induced by Bni1p serve as track for type V myosin that migrates towards the barbed ends to transport secretory vesicles that are needed for budding and polarized growth (*54–57*). This mechanism also seems to be involved in forming the proper orientation of the microtubule organization, as the myosin V (myo2p) was shown to move microtubules along the polarized actin cables, via its binding to Kar9/Bim1 complex (*54–57* and references therein and Fig. 3, upper panel). APC and EB1 have been postulated as mammalian orthologs for Kar9 and Bim1, respectively, and while the final proof has yet to come, it is expected that similar kinds of actin-based microtubule organization strategies are employed, under certain contexts, in highly polarized mammalian cells such as neurons, as well. Consistent with this notion, mDia1 affects orientation and the stability of microtubules in HeLa cells and has been shown to spatially coordinate actin polymerization and the stability of microtubule structures (*58*, *59*).

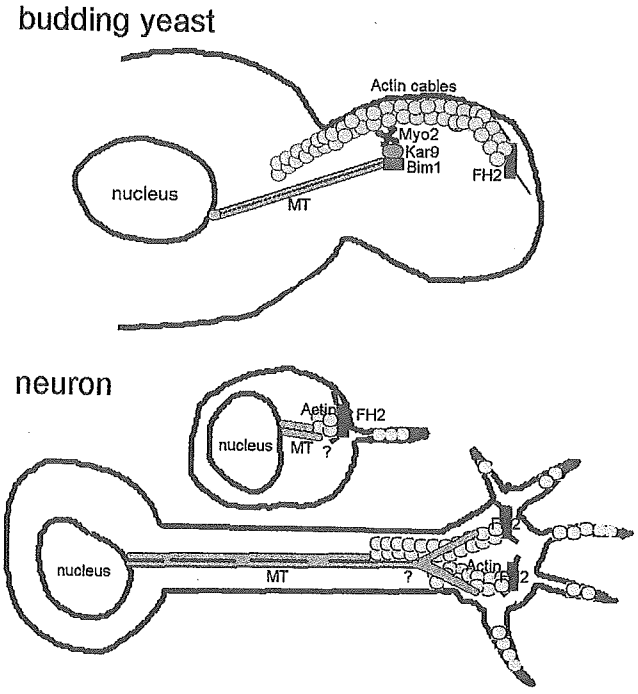

Fig. 3. **mDia may have a privileged role in assembling a cytoskeletal scaffold that links actin and microtubule structures, both in the yeast buds and in neuronal axons.** Upper panel: In the yeast, the FH2 (red rectangle)-containing formin Bni1p nucleates and assembles actin (yellow circles) cables which serve as track for myosin V motors. One of the cargo that the myosin V (Myo2) transports is the Kar9/Bim1 complex, which then is able to recruit microtubules (green rods) into the buds. Lower panel: FH2 domain (red rectangle) of mDia1 may exert a similar effect at the neck of an initiating axon or inside the growth cones. mDia1 nucleates and assembles actin (yellow circles) microfilaments, while probably also regulating microtubule (green rods) stability in a spatially coordinated fashion. However, the molecular identity of the scaffold that hinges together actin and microtubule structures remains to be identified. Furthermore, actin structures in the filopodia and lamellipodia present at the edge of a growth cone are likely to be assembled in a separate manner by distinct nucleators (red hexagone) such as e.g. Arp2/3.

As mDia proteins are most concentrated at the middle portion of the growth cones, an area where actin and microtubule cytoskeletons dynamically interact (*60*, *61*), it is tempting to speculate that mDia-driven remodeling of new F-actin bundles and coordinated microtubule arrays directs axon growth in a Rho-dependent manner, in a way that remains largely independent of the Arp2/3 complex-dependent lamellipodia and filopodia regulation

(*62*), at the tip and edge of the growing growth cones (Fig.3, lower panel). Further elucidation of the exact nature of the mDia-based neuronal cytoskeletal structures will certainly provide new insight to better understanding the molecular machinery allowing neurons to faithfully translate extracellular signals into orchestrated morphogenesis and faithful patterning that are critical for establishing a functional neuronal circuit.

My utmost thanks go to S. Narumiya, T. Furuyashiki, and Y. Arakawa, who were major contributors for the studies from which the model presented in this review was inspired. I apologize to the many authors whom I could not reference due to space limitations. I am also grateful to T. Kinbara for secretarial assistance. This work was supported in part by grants-in aid from the Ministry of Education, Culture, Sports, Science and Technology and the Ministry of Health, Labour and Welfare of Japan, and grants from PRESTO-Japan Science and Technology Corporation, the Tanabe Medical Frontier Conference, and Human Frontier Science Program.

REFERENCES

1. Goodman, C.S. and Shatz, C.J. (1993) Developmental mechanisms that generate precise patterns of neuronal connectivity. *Cell Suppl.* **72**, 77–98
2. da Silva, J.S. and Dotti, C.G. (2002) Breaking the neuronal sphere: regulation of the actin cytoskeleton in neuritogenesis. *Nat. Rev. Neurosci.* **3**, 694–704
3. Dingwell, K.S., Holt, C.E., and Harris, W.A. (2000) The multiple decisions made by growth cones of RGCs as they navigate from the retina to the tectum in *Xenopus* embryos. *J. Neurobiol.* **44**, 246–259
4. Culotti, J.G. and Kolodkin, A.L. (1996) Functions of netrins and semaphorins in axon guidance. *Curr. Opin. Neurobiol.* **6**, 81–88
5. Tessier-Lavigne, M., and Goodman, C.S. (1996) The molecular biology of axon guidance. *Science* **274**, 1123–1133
6. Van Vactor, D. and Flanagan, J.G. (1999) The middle and the end: slit brings guidance and branching together in axon pathway selection. *Neuron* **22**, 649–652
7. Huang, E.J. and Reichardt, L.F. (2001) Neurotrophins: roles in neuronal development and function. *Ann. Rev. Neurosci.* **24**, 677–736
8. Liu, B.P. and Strittmatter, S.M. (2001) Semaphorin-mediated axonal guidance via Rho-related G proteins. *Curr. Opin. Cell Biol.* **13**, 619–626
9. Tanaka, E. and Sabry, J. (1995) Making the connection: cytoskeletal rearrangements during growth cone guidance. *Cell* **83**, 171–176
10. Luo, L. (2002) Actin cytoskeleton regulation in neuronal morphogenesis and structural plasticity. *Annu. Rev. Cell. Dev. Biol.* **18**, 601–635
11. Narumiya, S., Ishizaki, T., and Watanabe, N. (1997) Rho effectors and reorganization of actin cytoskeleton. *FEBS Lett.* **410**, 68–72
12. Gallo, G. and Letourneau, P.C. (1998) Axon guidance: GTPases help axons reach their targets. *Curr. Biol.* **8**, R80–R82
13. Luo, L. (2000) Rho GTPases in neuronal morphogenesis. *Nat. Rev. Neurosci.* **1**, 173–180
14. Dickson, B.J. (2001) Rho GTPases in growth cone guidance. *Curr. Opin. Neurobiol.* **11**, 103–110
15. Nikolic, M. (2002) The role of Rho GTPases and associated kinases in regulating neurite outgrowth. *Int. J. Biochem. Cell Biol.* **34**, 731–745
16. Etienne-Manneville, S., and Hall, A. (2002) Rho GTPases in cell biology. *Nature* **420**, 629–635
17. Sebok, A., Nusser, N., Debreceni, B., Guo, Z., Santos, M.F., Szeberenyi, J., and Tigyi, G. (1999) Different roles for RhoA during neurite initiation, elongation, and regeneration in PC12 cells. *J. Neurochem.* **73**, 949–960
18. Bashaw, G.J., Hu, H., Nobes, C.D., and Goodman, C.S. (2001) A novel Dbl family RhoGEF promotes Rho-dependent axon attraction to the central nervous system midline in *Drosophila* and overcomes Robo repulsion. *J. Cell Biol.* **155**, 1117–1122
19. Billuart, P., Bienvenu, T., Ronce, N., des Portes, V., Vinet, M.C., Zemni, R., Roest, Crollius, H., Carrie, A., Fauchereau, F., Cherry, M., Briault, S., Hamel, B., Fryns, J.P., Beldjord, C., Kahn, A., Moraine, C., and Chelly, J. (1998) Oligophrenin-1 encodes a rhoGAP protein involved in X-linked mental retardation. *Nature* **392**, 923–926
20. Kutsche, K., Yntema, H., Brandt, A., Jantke, I., Nothwang, H.G., Orth, U., Boavida, M.G., David, D., Chelly, J., Fryns, J.P., Moraine, C., Ropers, H.H., Hamel, B.C., van Bokhoven, H., and Gal, A. (2000) Mutations in ARHGEF6, encoding a guanine nucleotide exchange factor for Rho GTPases, in patients with X-linked mental retardation. *Nat. Genet.* **26**, 247–250
21. Allen, K.M., Gleeson, J.G., Bagrodia, S., Partington, M.W., MacMillan, J.C., Cerione, R.A., Mulley, J.C., and Walsh, C.A. (1998) PAK3 mutation in nonsyndromic X-linked mental retardation. *Nat. Genet.* **20**, 25–30
22. Frangiskakis, J.M., Ewart, A.K., Morris, C.A., Mervis, C.B., Bertrand, J., Robinson, B.F., Klein, B.P., Ensing, G.J., Everett, L.A., Green, E.D., Proschel, C., Gutowski, N.J., Noble, M., Atkinson, D.L., Odelberg, S.J., and Keating, M.T. (1996) LIM-kinase1 hemizygosity implicated in impaired visuospatial constructive cognition. *Cell* **86**, 59–69
23. Tassabehji, M., Metcalfe, K., Fergusson, W.D., Carette, M.J., Dore, J.K., Donnai, D., Read, A.P., Proschel, C., Gutowski, N.J., Mao, X., and Sheer, D. (1996) LIM-kinase deleted in Williams syndrome. *Nature Genet* **13**, 272–273
24. Schenck, A., Bardoni, B., Langmann, C., Harden, N., Mandel, J.L., and Giangrande, A. (2003) CYFIP/Sra-1 controls neuronal connectivity in *Drosophila* and links the Rac1 GTPase pathway to the fragile X protein. *Neuron* **38**, 887–898
25. Bito, H., Furuyashiki, T., Ishihara, H., Shibasaki, Y., Ohashi, K., Mizuno, K., Maekawa, M., Ishizaki, T., and Narumiya, S. (2000) A critical role for a Rho-associated kinase, p160ROCK, in determining axon outgrowth in mammalian CNS neurons. *Neuron* **26**, 431–441
26. Arakawa, Y., Bito, H., Furuyashiki, T., Tsuji, T., Takemoto-Kimura, S., Kimura, K., Nozaki, K., Hashimoto, N., and Narumiya, S. (2003) Control of axon elongation via an SDF-1alpha / Rho/mDia pathway in cultured cerebellar granule neurons. *J. Cell Biol.* **161**, 381–391
27. Fournier, A.E., Takizawa, B.T., and Strittmatter, S.M. (2003) Rho kinase inhibition enhances axonal regeneration in the injured CNS. *J. Neurosci.* **23**, 1416–1423
28. Yuan, X.B., Jin, M., Xu, X., Song, Y.Q., Wu, C.P., Poo, M.M., and Duan, S. (2003) Signalling and crosstalk of Rho GTPases in mediating axon guidance. *Nat. Cell Biol.* **5**, 38–45
29. Threadgill, R., Bobb, K., and Ghosh, A. (1997) Regulation of dendritic growth and remodeling by Rho, Rac, and Cdc42. *Neuron* **19**, 625–634
30. Kimura, K., Ito, M., Amano, M., Chihara, K., Fukata, Y., Nakafuku, M., Yamamori, B., Feng, J., Nakano, T., Okawa, K., Iwamatsu, A., and Kaibuchi, K. (1996) Regulation of myosin phosphatase by Rho and Rho-associated kinase (Rho-kinase). *Science.* **273**, 245–248
31. Uehata, M., Ishizaki, T., Satoh, H., Ono, T., Kawahara, T., Morishita, T., Tamakawa, H., Yamagami, K., Inui, J., Maekawa, M., and Narumiya S. (1997) Calcium sensitization of smooth muscle mediated by a Rho-associated protein kinase in hypertension. *Nature* **389**, 990–994
32. Dontchev, V.D. and Letourneau, P.C. (2002) Nerve growth factor and semaphorin 3A signaling pathways interact in regulating sensory neuronal growth cone motility. *J. Neurosci.* **22**, 6659–6669
33. Watanabe, N., Madaule, P., Reid, T., Ishizaki, T., Watanabe, G., Kakizuka, A., Saito, Y., Nakao, K., Jockusch, B.M., and Narumiya, S. (1997) p140mDia, a mammalian homolog of *Dro-*